A new Jurassic lizard from China

Authors: Liping Dong, Yuan Wang, Lijie Mou, Guoze Zhang, and Susan E. Evans

Source: Geodiversitas, 41(16) : 623-641

Published By: Muséum national d'Histoire naturelle, Paris

URL: https://doi.org/10.5252/geodiversitas2019v41a16

BioOne Complete (complete.BioOne.org) is a full-text database of 200 subscribed and open-access titles in the biological, ecological, and environmental sciences published by nonprofit societies, associations, museums, institutions, and presses.

Your use of this PDF, the BioOne Complete website, and all posted and associated content indicates your acceptance of BioOne's Terms of Use, available at www.bioone.org/terms-o-use.

Usage of BioOne Complete content is strictly limited to personal, educational, and non - commercial use. Commercial inquiries or rights and permissions requests should be directed to the individual publisher as copyright holder.

BioOne sees sustainable scholarly publishing as an inherently collaborative enterprise connecting authors, nonprofit publishers, academic institutions, research libraries, and research funders in the common goal of maximizing access to critical research.

Downloaded From: https://bioone.org/journals/Geodiversitas on 18 Nov 2019
Terms of Use: https://bioone.org/terms-of-use Access provided by University College London

A new Jurassic lizard from China

Liping DONG
Yuan WANG
Key Laboratory of Vertebrate Evolution and Human Origins of the Chinese Academy of Sciences,
Institute of Vertebrate Paleontology and Paleoanthropology, Chinese Academy of Sciences,
142 Xi-Zhi-Men-Wai St, P.O. Box 643, Beijing 100044 (China)
and CAS Center for Excellence in Life and Paleoenvironment,
142 Xi-Zhi-Men-Wai St, P.O. Box 643, Beijing 100044 (China)
dongliping@ivpp.ac.cn (corresponding author)

Lijie MOU
Guoze ZHANG
Fossil Protection Office, Jianping Bureau of Land and Resources, Jianping, 122400 (China)

Susan E. EVANS
Department of Cell and Developmental Biology, University College London, Gower Street,
London, WC1E 6BT (United Kingdom)

Submitted on 24 January 2019 | accepted on 31 July 2019 | published on 13 September 2019

urn:lsid:zoobank.org:pub:D6AEA459-651C-4E73-AA82-89739193D783

Dong L., Wang Y., Mou L., Zhang G. & Susan E. Evans 2019. — A new Jurassic lizard from China, *in* Steyer J.-S., Augé M. L. & Métais G. (eds), Memorial Jean-Claude Rage: A life of paleo-herpetologist. *Geodiversitas* 41 (16): 623-641. https://doi.org/10.5252/geodiversitas2019v41a16. http://geodiversitas.com/41/16

ABSTRACT
The Jurassic record of lizards in eastern Asia is poor by comparison with that of the Cretaceous. In China, to date, the only confirmed records from this period are an armoured lizard from Shishugou, Xinjiang Uygur Autonomous Region, of probable Oxfordian age, and two unnamed juvenile specimens from the slightly older, Callovian-Oxfordian, Daohugou locality of Nei Mongol. Here we describe the first lizard from the locality of Guancaishan, Jianping County, Liaoning Province. This locality is close to Daohugou, and is considered t o be of similar age. The new skeleton is articulated and well-preserved. It is distinguished from other Jurassic-Cretaceous lizards by a unique combination of derived characters, notably a long frontal with posterior processes that clasp the short parietal; cranial osteoderms limited to the lower temporal and supraocular regions; and an elongated manus and pes. Phylogenetic analysis using morphological data alone places the new taxon on the stem of a traditional 'Scleroglossa', but when the same data is run with a backbone constraint tree based on molecular data, the new taxon is placed on the stem of Squamata as a whole. Thus its position, and that of other Jurassic and Early Cretaceous taxa, seem to be influenced primarily by the position of Gekkota.

KEY WORDS
Lizard,
Jurassic,
Guancaishan locality,
China,
phylogenetic analysis,
new genus,
new species.

Downloaded From: https://bioone.org/journals/Geodiversitas on 18 Nov 2019
Terms of Use: https://bioone.org/terms-of-use Access provided by University College London

RÉSUMÉ
Un nouveau lézard du Jurassique de Chine.
Le registre jurassique des lézards d'Asie orientale est pauvre en comparaison de celui du Crétacé. En Chine, à ce jour, les seuls enregistrements confirmés pour cette période sont un lézard à armure du Shishugou, région autonome ouïgoure du Xinjiang, d'âge probable oxfordien, et deux spécimens juvéniles non nommés et légèrement plus vieux, d'âge callovien-oxfordien, de la localité de Daohugou en Mongolie intérieure. Nous décrivons ici le premier lézard de la localité de Guancaishan, comté de Jianping, province du Liaoning. Cette localité, proche de Daohugou, est considérée comme étant du même âge. Le nouveau squelette est articulé et bien conservé. Il se distingue des autres lézards jurassiques-crétacés par une association unique de caractères dérivés, notamment un long frontal avec des processus postérieurs qui enserrent le court pariétal ; des ostéodermes crâniens limités aux régions temporales et supraoculaires inférieures ; et des mains et des pieds allongés. L'analyse phylogénétique, basée uniquement sur des données morphologiques, place le nouveau taxon à la base du traditionnel 'Scleroglossa', mais lorsque la même analyse est réalisée avec une contrainte de type 'backbone' basée sur les données moléculaires, le nouveau taxon se place à la base de l'ensemble des Squamata. De fait, sa position et celle des autres taxa jurassiques et crétacés inférieurs semblent influencéee principalement par la position des Gekkota.

MOTS CLÉS
Lézard,
Jurassique,
localité de Guancaishan,
Chine,
analyse phylogénétique,
genre nouveau,
espèce nouvelle.

INTRODUCTION

The Cretaceous fossil record of lizards in China is comparatively good, with several genera known from the Jehol Biota and its equivalents (e.g. *Yabeinosaurus* Endo & Shikama, 1942 [Endo & Shikama 1942; Young 1958; Ji *et al.* 2001; Evans *et al.* 2005; Evans & Wang 2012; Dong *et al.* 2017], *Dalinghosaurus* Ji, 1998 [Ji 1998; Ji & Ji 2004; Evans & Wang 2005; Evans *et al.* 2007], *Liushusaurus* Evans & Wang, 2010 [Evans & Wang 2010], *Mimobecklesisaurus* Li, 1985 [Li 1985], *Xianglong* Li, Gao, Hou & Xu, 2007 [Li *et al.* 2007], *Pachygenys* Gao & Cheng, 1999 [Gao & Cheng 1999]) and many others from the Late Cretaceous of Jiangxi (e.g. Lü *et al.* 2008; Mo *et al.* 2010, 2012) and Henan (Xu *et al.* 2014) provinces, and of the Nei Mongol Autonomous Region (Inner Mongolia) (e.g. Gao & Hou 1995, 1996; Wu *et al.* 1996; Dong *et al.* 2018). However, the Jurassic lizard record is currently limited to a few localities centered on two areas, Daohugou in Nei Mongol, and the Junggar Basin of the Xinjiang Uygur Autonomous Region. Although the Daohugou deposits are sometimes reported to be of Middle Jurassic age (e.g. Ji *et al.* 2006), the current consensus (Sullivan *et al.* 2014; Zhou & Wang 2017) is that they lie at the Middle-Upper Jurassic boundary (Callovian-Oxfordian). Two articulated lizard, or lizard-like, specimens, both juvenile, have been described from Daohugou. One is represented mainly by skin impressions (Evans & Wang 2007). The other has some visible bones as thin, dark shapes (Evans & Wang 2009). Although these two specimens clearly represent different taxa (e.g. based on body proportions), their poor preservation and immaturity preclude either naming or a detailed assessment of phylogenetic position. A more complete lizard skeleton has been recovered from the early Late Jurassic (Oxfordian) Shishugou Formation in the central Junggar Basin of Xinjiang. To date, this important specimen has been reported briefly in an abstract (Conrad *et al.* 2013) as having vomerine teeth, a rectangular frontal, incipient cusps on the marginal teeth, long-limbs, and a body covering of osteoderms. A detailed description is in progress (James M. Clark, pers. comm.). More fragmentary lizard remains, in the form of small dentary fragments and rectangular osteoderms, were reported by Richter *et al.* (2010) from the lower part of the Qigu Formation at Liuhuanggou at the southern edge of the Junggar Basin. Richter *et al.* (2010) attributed these remains to the Paramacellodidae, a stem-scincoid group known from several Jurassic-Cretaceous localities around the world (Estes 1983), including China (Early Cretaceous *Mimobecklesisaurus* Li, 1985).

Here we describe a new lizard from a locality named as Guancaishan ('Coffin Mount'), Liaoning Province. These deposits are generally considered to be close in age to the Daohugou Beds (Sullivan *et al.* 2014), and of late Middle Jurassic (Callovian) or, more likely, of early Late Jurassic (Oxfordian) age.

GEOLOGY AND MATERIAL

The new specimen comprises a part and counterpart bearing the complete skeleton of a small lizard from the Guancaishan locality and is catalogued in the collections of the Jianping County Museum as HS-0001. The Guancaishan locality (41°24.373'N, 119°26.995'E) is 1.2 km northeast of Muyingzi Village, Shahai Town, Jianping County, Liaoning Province (Fig. 1). The fossil was discovered in silicified dark mudstone on the southern slope of an isolated local mountain shaped like a coffin (Guancaishan means "Coffin Mount" in Chinese Pinyin). The site has also yielded several specimens of the putative salamandroid *Beiyanerpeton* Gao & Shubin, 2012 (Gao & Shubin 2012) as well as more than 400 fully articulated specimens of the cryptobranchid

Downloaded From: https://bioone.org/journals/Geodiversitas on 18 Nov 2019
Terms of Use: https://bioone.org/terms-of-use Access provided by University College London

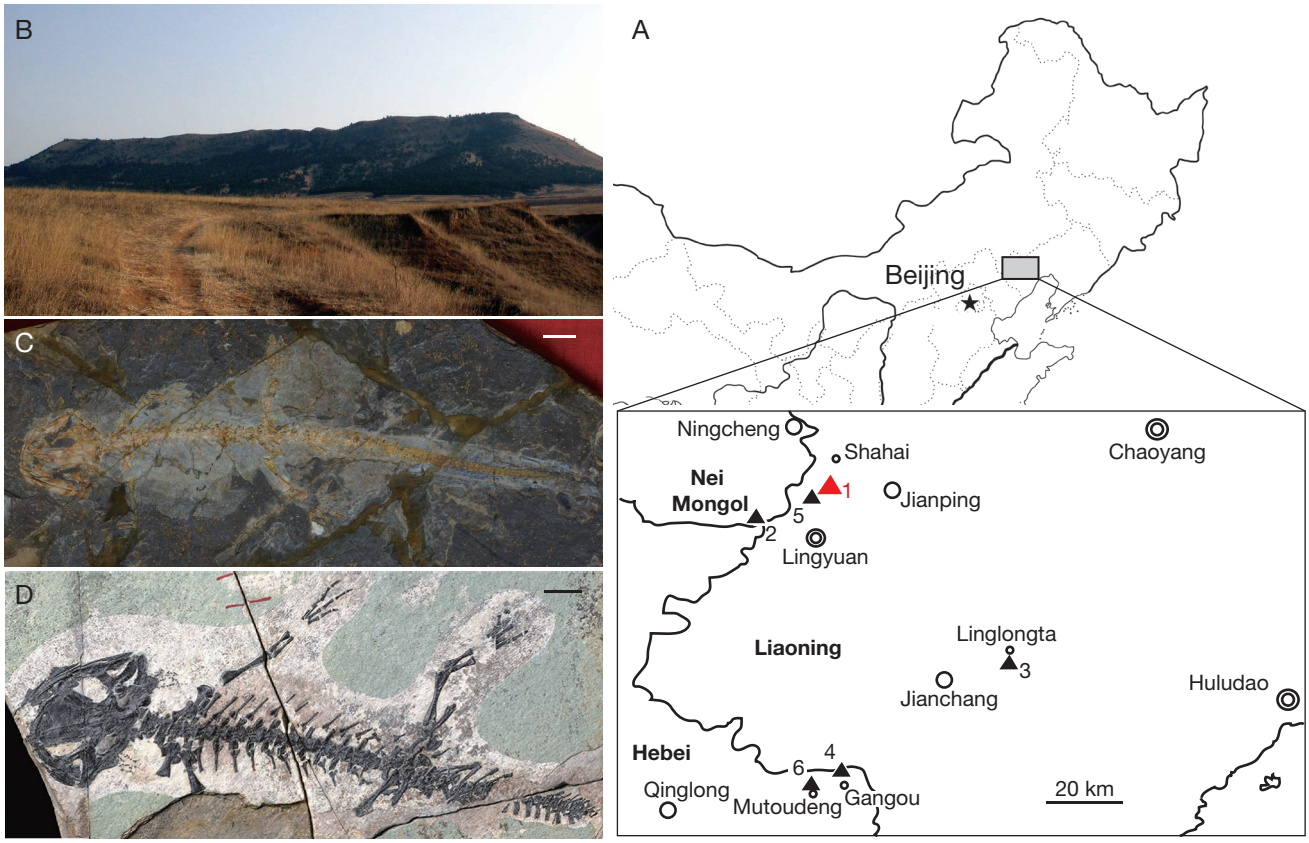

FIG. 1. — The Guancaishan locality: **A**, map showing the location of the Guancaishan locality, with an enlargement of the area where the Daohugou Biota is distributed. The triangles show the Daohugou Biota localities (details see Sullivan *et al.* [2014]): **1**, Guancaishan locality; **2**, Daohugou locality; **3**, Daxishan locality; **4**, Zhuanshanzi locality; **5**, Wubaiding locality; **6**, Bawanggou locality; **B**, Guancaishan ('Coffin Mount') locality seen in the distance showing its distinctive profile; **C**, *Chunerpeton tianyiensis* Gao & Shubin, 2003 specimen (IVPP V 15521) with polydactyly from Guancaishan locality (Wang *et al.* 2016); **D**, *Beiyanerpeton jianpingensis* Gao & Shubin, 2012 holotype from Guancaishan locality (Gao & Shubin 2012).

salamander *Chunerpeton tianyiensis* Gao & Shubin, 2003 (Zhang 2008; Sullivan *et al.* 2014; Han *et al.* 2016; Zhou & Wang 2017), many with soft body outlines. Wang *et al.* (2016) documented the first evidence of polydactyly in a Mesozoic caudate (*Chunerpeton* Gao & Shubin, 2003) based on five specimens from the Guancaishan site and nine from adjacent ones. Sullivan *et al.* (2014) proposed that *Chunerpeton tianyiensis* represented a common element linking the different localities in this area (southeastern Inner Mongolia [Nei Mongol], northern Hebei and western Liaoning) that have yielded the Daohugou Biota. They considered the Daohugou Biota horizons to be situated stratigraphically near the boundary between the Jiulongshan (Middle Jurassic, Callovian) and Tiaojishan (Upper Jurassic, Oxfordian) formations, and tentatively referred the fossil-bearing strata at Guancaishan to the Tiaojishan (Lanqi) Formation. Gao & Shubin (2012) and Huang *et al.* (2016) came to the same conclusion, although Zhou & Wang (2017) proposed the term Yanliao Biota to include fossil assemblages from both the Jiulongshan (or Haifanggou) and Tiaojishan (or Lanqi) formations, making no distinction between them. The present paper follows Sullivan *et al.* (2014). The lava layer well-above the fossil bed has a U-PB SHRIMP date of 157±3 Ma (Liu *et al.* 2006), so the fossil bed must be older than this.

In addition to the lizard and salamander specimens, the Guancaishan deposits have yielded plants; insects and conchostracans; and rare pterosaur material. These specimens are preserved in tuffaceous mudstones and shales interposed between thicker layers of volcanic rocks. The plants and animals found in the deposits lived in and around a lake that was frequently contaminated by volcanic ash and other material.

The lizard specimen comprises a compressed part and counterpart on a relatively thin slab of matrix, precluding standard micro-CT scanning (Figs 2-6). However, the skull in each specimen (part and counterpart) was scanned using a 160KV Micro-Computer Laminography system (developed by the Institute of High Energy Physics [IHEP], Chinese Academy of Sciences [CAS]) at the Key Laboratory of Vertebrate Evolution and Human Origins, CAS with a resolution of 16.3371 µm (Liu *et al.* 2015). Although this does not permit segmentation, it did permit us to scroll down below the surface layer in order to reveal some additional details of the palate, braincase and dentition that are not visible from the surface (Fig. 7; Appendix 3).

Downloaded From: https://bioone.org/journals/Geodiversitas on 18 Nov 2019
Terms of Use: https://bioone.org/terms-of-use Access provided by University College London

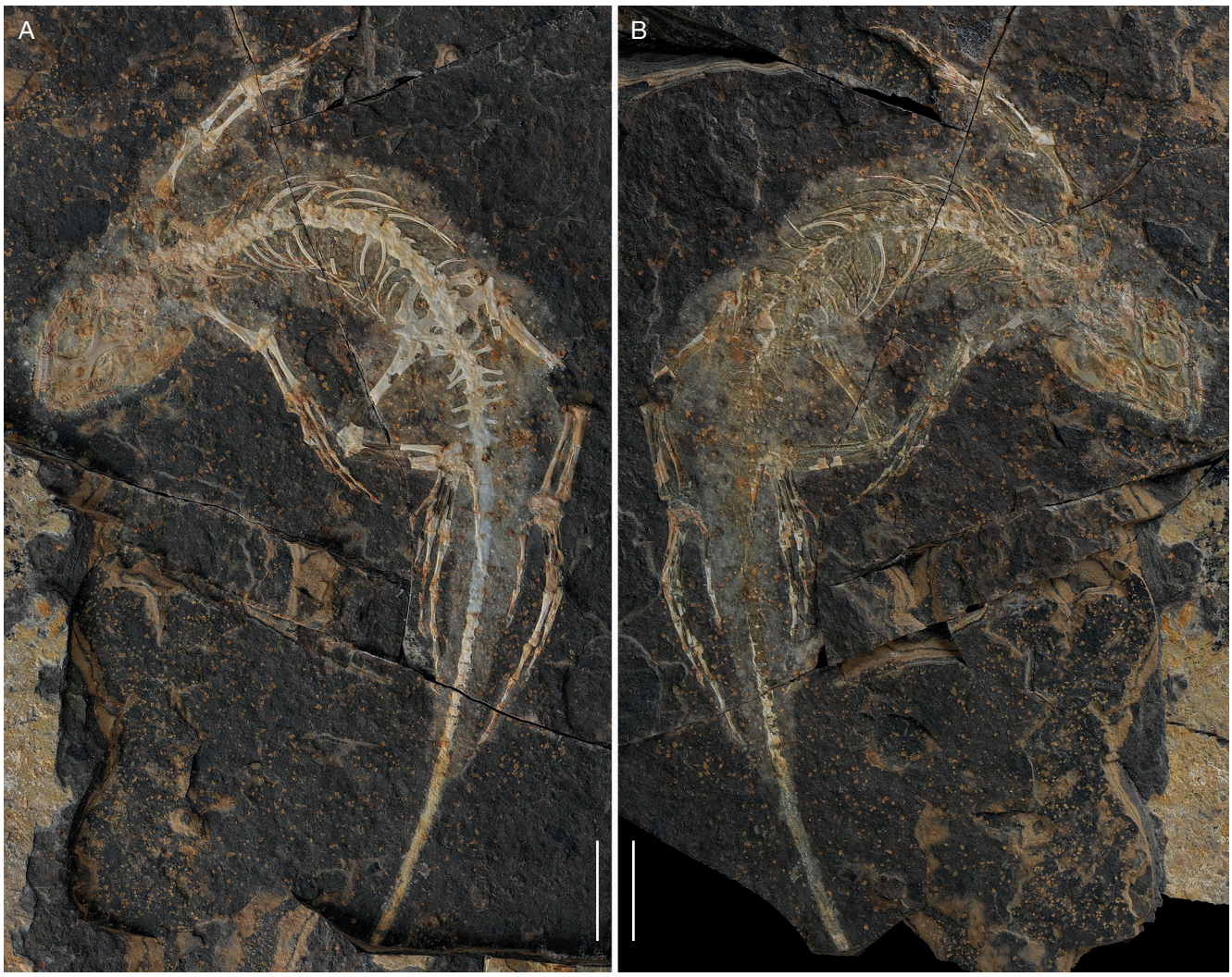

FIG. 2. — *Hongshanxi xiei* n. gen., n. sp., holotype, Jianping County Museum, HS-0001: **A**, the main part block; **B**, the counterpart block. Scale bars: 10 mm.

SYSTEMATIC PALAEONTOLOGY

Order SQUAMATA Oppel, 1811

Hongshanxi n. gen.

urn:lsid:zoobank.org:act:F194AB36-3335-46A7-A5DD-4AD93E52361B

TYPE SPECIES. — *Hongshanxi xiei* n. sp.

ETYMOLOGY. — The Hongshan culture is an ancient (5000 BP) culture centred close to Jianping, near the fossil locality. "xi"refers to "蜥" in Chinese, meaning a lizard.

DIAGNOSIS. — As for type species.

Hongshanxi xiei n. sp.
(Figs 1-7)

urn:lsid:zoobank.org:act:838578B0-E550-4498-B541-6612FBA25A6C

TYPE SPECIMEN. — Jianping County Museum, HS-0001 (Fig. 2), the part and counterpart of a small block bearing a complete lizard specimen.

TYPE LOCALITY AND HORIZON. — Guancaishan (41°24.373'N, 119°26.995'E), 1.2 km northeast of Muyingzi Village, Shahai Town, Jianping County, Liaoning Province; Tiaojishan (Lanqi) Formation; Oxfordian, Jurassic.

ETYMOLOGY. — The species name honours Mr. Xie Jingguo who recovered the fossil.

DIAGNOSIS. — Small-bodied lizard characterized by the following unique combination of features that distinguishes it from all known Mesozoic taxa: elongate fused frontal with trifurcate posterior border that clasps anterior and lateral margins of the parietal; short parietal; nasals fused at least posteriorly; robust jugal meets prefrontal and excludes maxilla from orbital margin; jugal contacts squamosal in upper temporal bar to exclude postorbital from lower temporal fenestra; squamosal with strongly hooked posteroventral process; lower temporal fenestra covered by large thin osteoderms of varying size; osteoderms in supraocular scales; no continuous osteoderm covering of skull surface or body; manus longer than humerus+radius; pes longer than femur+tibia.

Downloaded From: https://bioone.org/journals/Geodiversitas on 18 Nov 2019
Terms of Use: https://bioone.org/terms-of-use Access provided by University College London

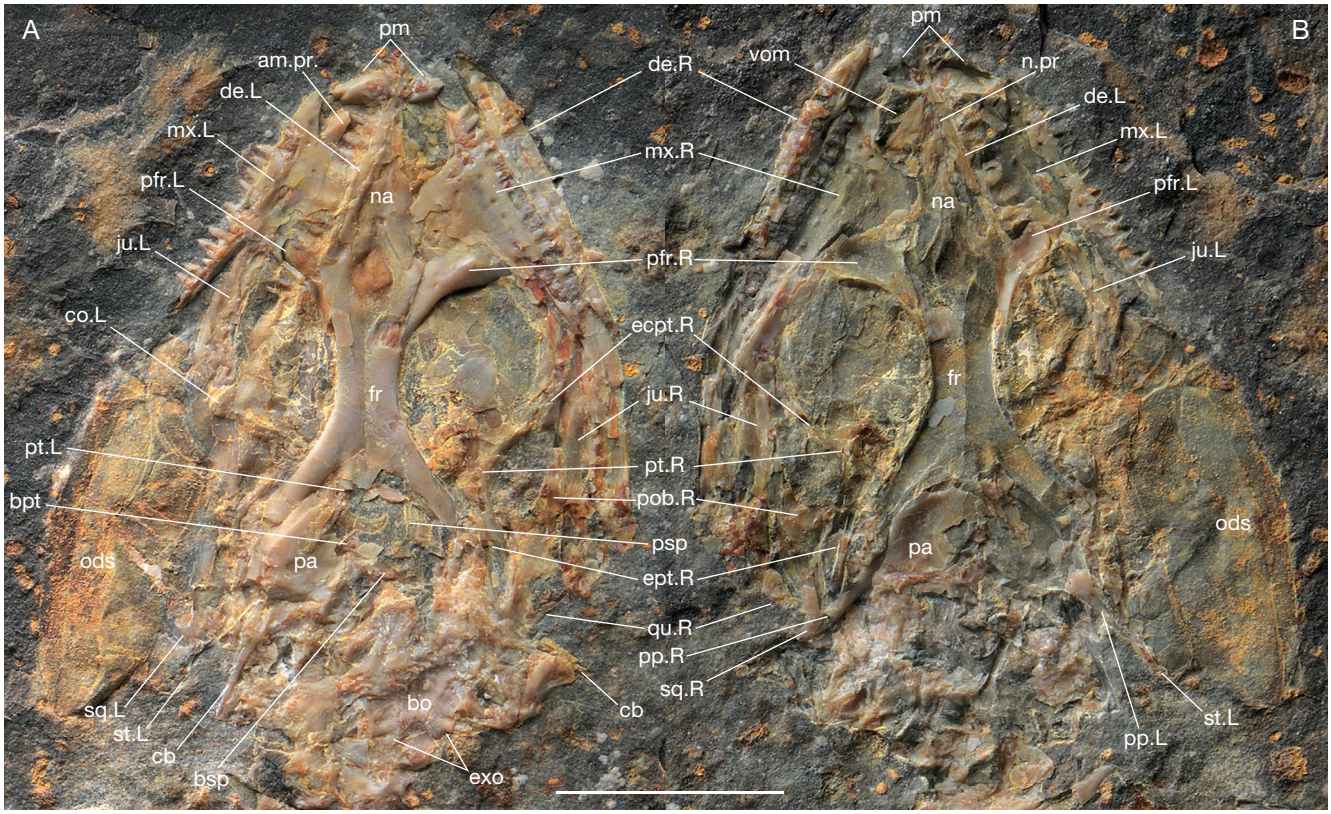

FIG. 3. — *Hongshanxi xiei* n. gen., n. sp., skull in dorsal view from main block (**A**) and counterpart block (**B**). Abbreviations: **am.pr.**, anteromedial process of maxilla; **bo**, basioccipital; **bpt**, basipterygoid process; **bsp**, basisphenoid; **cb**, ceratobranchial; **co.L**, left coronoid; **de.L**, left dentary; **de.R**, right dentary; **ecpt.R**, right ectopterygoid; **ept.R**, right epipterygoid; **exo**, exoccipital/opisthotic; **fr**, frontal; **ju.L**, left jugal; **ju.R**, right jugal; **mx.L**, left maxilla; **mx.R**, right maxilla; **na**, nasal; **n.pr**, nasal process of premaxilla; **ods**, osteoderms; **pa**, parietal; **pm**, premaxilla; **pfr.L**, left prefrontal; **pfr.R**, right prefrontal; **pob.R**, right postorbital; **pp.L**, left postparietal process; **pp.R**, right postparietal process; **psp**, parasphenoid; **pt.L**, left pterygoid; **pt.R**, right pterygoid; **qu.R**, right quadrate; **sq.L**, left squamosal; **sq.R**, right squamosal; **st.L**, left supratemporal; **vom**, vomer. Scale bar: 5 mm.

DESCRIPTION

The holotype specimen of *Hongshanxi xiei* n. gen., n. sp. represents a small lizard, preserved in dorsal view, with a snout-pelvis length (SPL) of 55 mm (Fig. 2). Most of the bone is on the main part, but some details of the temporal bones, osteoderms, and pectoral girdle are provided by the counterpart. The individual was skeletally immature at death, as evidenced by the incomplete mineralization of the epiphyses, unfused pelvic elements, the separate olecranon, and the nearly fused astragalocalcaneum, but the well-formed skull sutures and postcranial elements suggest that the animal was probably subadult rather than juvenile.

Skull

The skull is 15 mm in length and is relatively well-preserved, with most detail on the main block (Fig. 3A) and some on the counterpart (Fig. 3B). None of the skull bones bears any trace of ornamentation. The external nares are large and dorsoventrally deep. The orbits are also large and ovoid. They appear to be partially covered by thin osteoderms that probably lay below the supraocular scales. The upper temporal fenestra is narrow and rather small. The lower temporal fenestra is larger and, like the orbit, appears to be covered by a mosaic of large thin osteodermal plates. However, there is no indication that the rest of the skull was covered in this way.

Nasal. Each nasal has a slender posterior tab that fits into an anterolateral frontal recess, but anterior to the frontal the nasals meet and appear to fuse in the midline. The nasals seem to taper anteriorly but whether they remain fused anteriorly is unclear as this region is damaged.

Premaxilla. Compression of the skull has pushed the left mandible under the rostrum and through the premaxilla and the anterior part of the nasals (Fig. 3A). As a result, the premaxilla has been broken into two unequal parts. Had the premaxilla been paired, it is likely that the two parts would have separated cleanly under compression, rather than breaking through one of the rami. However, there seem to be two long, slender nasal processes separated from the alveolar plate of the premaxilla(e), as seen more clearly on the CT scan images of the counterpart (Fig. 7; Appendix 3). Therefore it is possible that the premaxillae were paired in the juvenile and were in the process of fusing from ventral to dorsal. The nasal process is similar in length to the total width of the alveolar plate of the premaxilla. The scan images of the main part block show more of the premaxillary dentition, with at least eight pleurodont tooth positions of similar size to those on the maxilla (Appendix 3). However, due to the damage to the central region of the bone, it is not possible to

Downloaded From: https://bioone.org/journals/Geodiversitas on 18 Nov 2019
Terms of Use: https://bioone.org/terms-of-use Access provided by University College London

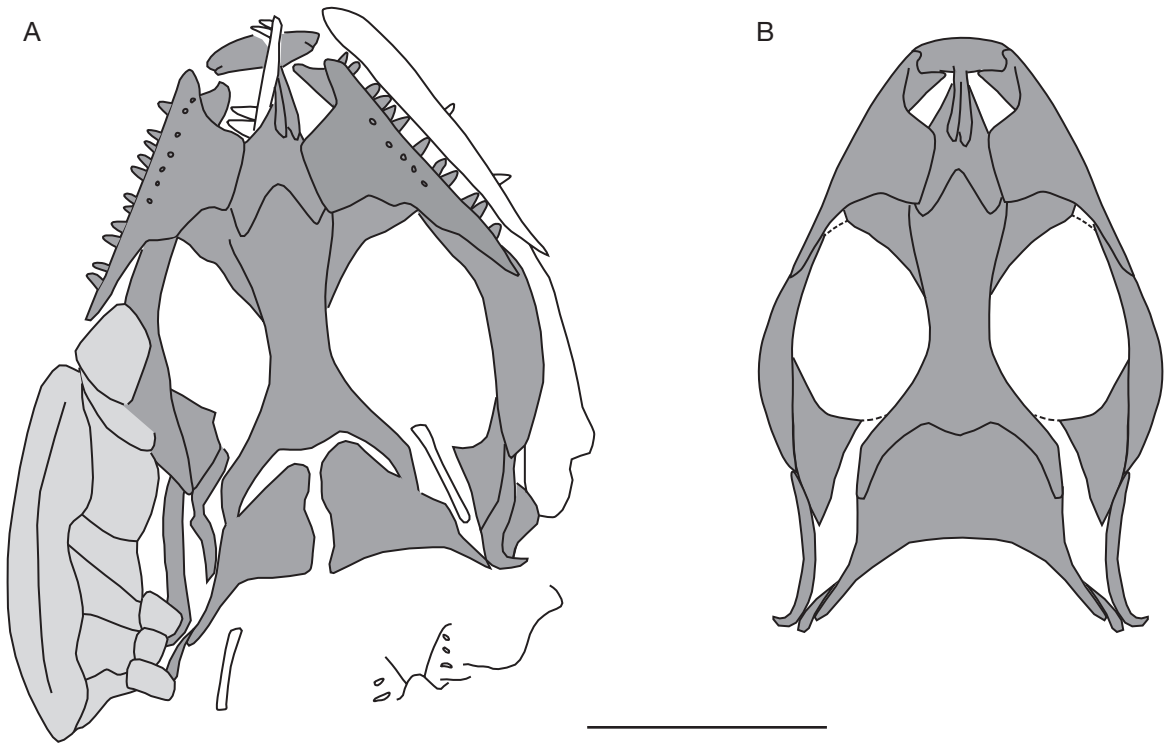

FIG. 4. — *Hongshanxi xiei* n. gen., n. sp.: **A**, line drawing of the skull, as preserved, in dorsal view based on both main and counterpart blocks. Temporal osteoderms are shown in light grey; ventral elements (right lower jaw, hyoid ceratobranchials, braincase [exoccipitals, basioccipital, otic capsule]) shown in outline; **B**, reconstruction of the skull in dorsal view. As the postoribtal region is compressed with the palatal and lower jaw pushing through it, the presence or absence of a separate postfrontal bone is uncertain. Dashed lines have therefore been used to complete the postorbital bar. Scale bar: 5 mm.

determine whether a median tooth was present. Bilaterally, the premaxilla bears recessed facets for the maxillae. Based on the scanned images (Appendix 3), the palatal plate of the premaxilla seems to be at least moderately developed and articulated with the medial branch of the maxillary anterior process.

Frontal. In the dorsal midline, the most characteristic element is the large frontal. Although there is a linear groove along the main axis, this does not appear to be a suture as it does not bisect the bone into equal parts and seems to be a combination of a midline groove and both anterior and posterior cracks. The bone is relatively narrow between the orbits and expands anteriorly and posteriorly. The anterior margin appears to be trifurcate, with a broad central triangular process and smaller lateral processes separated by recesses for the nasals. The posterior margin of the frontal is also, unusually, trifurcate. It has a broad median tab and two long lateral processes. These overlap the anterior and anterolateral margins of the parietal, lying within recesses along the lateral edges of the parietal. There is no obvious facet for a postfrontal seen on the frontal, but this may lie ventrolaterally. The CT scan images show that the crista cranii (sub-olfactory processes) are shallow and not fused in the ventral midline.

Parietal. The parietal is thin and is partly obscured by broken pieces of the braincase. Although the left side of the parietal is mostly preserved on the part block and the right side is on the counterpart block, the fact that the bone extends across the midline on the counterpart block suggests that it was originally single. The body of the parietal was short by comparison with the frontal (less than half the frontal length), and there is no obvious parietal foramen. As described above, the parietal has an unusual articulation with the frontal such that the body of the bone enters the margin of the upper temporal fenestra for a limited distance. Moreover, there are impressions of paired parietal tabs on either side of the midline, bracing the fronto-parietal articulation. A portion of the posterior, nuchal, margin of the parietal is preserved on the left side (main block, Fig. 3A) and appears shallow and vertical in orientation. The postparietal processes (counterpart block, Fig. 3B) are shorter than the body of the bone, tapered at the tip, and posterolaterally directed.

Maxilla. The maxilla is well preserved on both sides of the skull (Fig. 3A, B). It has a short premaxillary process, a large facial process with a horizontal rather than tapering dorsal margin, and a posterior process that extends just short of the mid-length of the orbit. The premaxillary process bears a lateral ramus that tapers to a tip in lateral view and fits into the recess on the corresponding premaxilla. Dorsally, the rectangular facial process overlaps the edge of the nasal; posteriorly it broadly overlaps the prefrontal, and just reaches the anterolateral process of the frontal. The palatal shelf of the maxilla seems well developed. Its anterior part, the

Downloaded From: https://bioone.org/journals/Geodiversitas on 18 Nov 2019
Terms of Use: https://bioone.org/terms-of-use Access provided by University College London

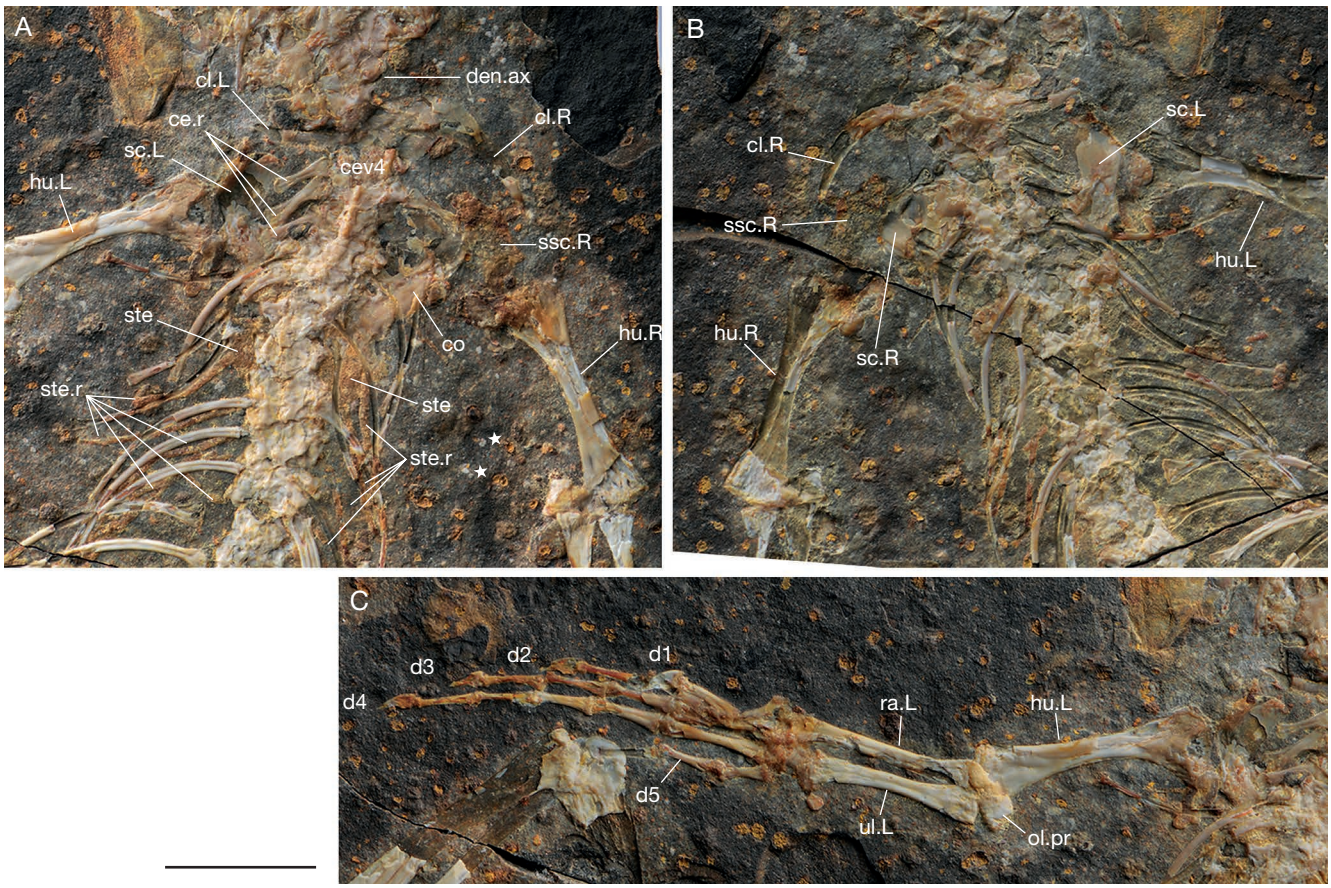

FIG. 5. — *Hongshanxi xiei* n. gen., n. sp., pectoral girdle and forelimb: **A**, midbody and pectoral girdle, main block; **B**, midbody and pectoral girdle, counterpart block; **C**, left forelimb, main block. Abbreviations: **ce.r**, cervical ribs; **cev4**, fourth cervical vertebra; **cl.L**, left clavicle; **cl.R**, right clavicle; **co**, coracoid; **d1**-**d5**, digits 1-5; **den.ax**, dens of the axis; **hu.L**, left humerus; **hu.R**, right humerus; **ol.pr**, detached olecranon process; **ra.L**, left radius; **sc.L**, left scapula; **sc.R**, right scapula; **ssc.R**, right suprascapula; **ste**, cartilage sternum; **ste.r**, sternal ribs; **ul.L**, left ulna. Scale bar: 5 mm.

medial process of the premaxillary process meets the palatal shelf of the premaxilla and, together with the lateral process, forms a dorsal depression. The teeth are homodont, simple cones with sharp tips. The left maxilla has 16 or 17 tooth positions, of which 12 are filled and another four contain immature replacement teeth; the right maxilla has 17 tooth positions of which 13 are filled and at least three contain small replacements.

Jugal. The left jugal is preserved in lateral view on the main block, the right is seen in medial view on the counterpart. It is a large, laterally compressed, element with a relatively deep suborbital process that sat in a shallow groove on the shallow posterior process of the maxilla, excluding the maxilla from the orbital margin and meeting the prefrontal anteriorly. The postorbital process is slightly wider than the suborbital process and meets it at an oblique angle. The posteroventral border of the postorbital process is thin by comparison with the thickened anterodorsal border. The medial view on the counterpart reveals the presence of a low median ridge. Dorsally, the jugal articulates with the postorbital and has a small contact with the tip of the squamosal. The postorbital bar is thus complete.

Prefrontal. The prefrontal is large and convex. Its anterolateral surface is covered by the facial process of the maxilla, but beneath the maxilla, the prefrontal also has a contact with the nasal. Ventromedially, the prefrontal may have met the tip of the jugal, and/or a lacrimal bone. The frontal process does not extend beyond the mid-orbit. Along the anterior margin of the orbit, the bone develops a weak ridge.

Lacrimal. There seems to be a separate bone between the prefrontal and maxilla on the right side, based on the scan images of the part block (Appendix 3), which might correspond to the lacrimal, and between this bone and the prefrontal is a foramen that we tentatively interpret as a lacrimal foramen.

Postfrontal and Postorbital. The posterodorsal corner of the orbit is difficult to resolve because of the supraocular osteoderms and both palatal and jaw elements that have pushed through from the underside. The postorbital (or possibly postorbitofrontal) is clearest on the counterpart block. It is roughly triangular, with a curved anterior orbital margin (forming roughly 35-40% of the posterior orbital border) and a tapering body that fills the anterior part of the upper temporal fenestra, reaching roughly one third of the length

Downloaded From: https://bioone.org/journals/Geodiversitas on 18 Nov 2019
Terms of Use: https://bioone.org/terms-of-use Access provided by University College London

TABLE 1. — Measurements of some squamates, *Hongshanxi xiei* n. gen., n. sp., *Yabeinosaurus robustus* Dong, Wang & Evans, 2017, *Dalinghosaurus longidigitus* Ji, 1998, and *Liushusaurus acanthocaudata* Evans & Wang, 2010, from the Daohugou and Jehol Biotae of China. Abbreviations: **SPL**, snout-pelvis length; **HuL**, humerus length; **RaL**, radius length; **HdL**, hand length; **FeL**, femur length; **TiL**, tibia length; **FtL**, foot length; **FLL**, forelimb length; **HLL**, hindlimb length.

Taxa	Measurements (mm)							FLL/ SPL	HuL/ SPL	RaL/ SPL	HdL/ SPL	HLL/ SPL	FeL/ SPL	TiL/ SPL	FtL/ SPL	Reference
	SPL	HuL	RaL	HdL	FeL	TiL	FtL									
H. xiei n. gen., n. sp., Jianping County Museum, HS-0001	55.0	8.0	5.8	14.4	13.3	9.2	24.0	51.3%	14.5%	10.5%	26.2%	84.5%	24.2%	16.7%	43.6%	this paper
Daohugou lizard 1, IVPP V 14386	43.7	4.9	5.2	6.6	7.0	8.8	9.2	38.2%	11.2%	11.9%	15.1%	57.2%	16.0%	20.1%	21.1%	Evans & Wang (2007, 2009)
Daohugou lizard 2, IVPP V 13747	60.1	8.5	6.8	12.5	12.7	10.4	16.8	46.3%	14.1%	11.3%	20.8%	66.4%	21.1%	17.3%	28.0%	Evans & Wang (2009)
Y. robustus, IVPP V 13284	180.0	18.5	8.5	23.4	23.4	21.6	36.0	28.0%	10.3%	4.7%	13.0%	45.0%	13.0%	12.0%	20.0%	Evans & Wang (2009)
D. longidigitus, IVPP V 14234.2	87.8	13.0	8.7	15.5	20.8	17.3	40.6	42.4%	14.8%	9.9%	17.7%	89.6%	23.7%	19.7%	46.2%	Evans *et al.* (2005, 2007)
D. longidigitus, IVPP V 13281	142.0	15.2	10.3	19.9	24.1	25.6	54.0	32.0%	10.7%	7.3%	14.0%	73.0%	17.0%	18.0%	38.0%	Evans & Wang (2009)
L. acanthocaudata, IVPP V 15587	66.0	9.0	6.3	9.3	11.1	8.4	13.4	37.3%	13.6%	9.5%	14.1%	49.8%	16.8%	12.7%	20.3%	Evans & Wang (2010)

of the squamosal. However, whether the postorbital met the frontal directly or there was an intervening postfrontal is not known. There is a bone fragment between the postorbital and skull roof on the left side of the skull (Figs 3; 4A), but it is not clear whether this is a slender postfrontal, or part of a jaw or palatal element that has been pushed dorsally. The reconstruction (Fig. 4B) therefore shows this region with a dashed line.

Squamosal. The squamosal is preserved on both sides, with the left bone on the main block and the right bone on the counterpart. It has a relatively long tapering anterior body that articulates dorsally with the postorbital and meets the jugal at its tip. The posterior tip has a strong ventral hook that presumably met a pit in the quadrate, and a slight dorsal expansion where the bone probably met the postparietal process of the parietal. A slender bone fragment distal to the (anatomical) left postparietal process (Figs 3; 4; 7; Appendix 3) may be a supratemporal.

Quadrate. Neither block shows the quadrate clearly, but part of the right bone may be present. The right postorbital and squamosal are mostly preserved on the counterpart, and there is a quadrate-shaped impression with a little of the tympanic crest preserved lateral to the squamosal. In the same position on the part block, the impressions of the postorbital and squamosal are clearly visible and they are associated with a mass of bone that represents fragments of the right quadrate. This mass is located ventral to the postorbital and squamosal, and lateral to the pterygoid quadrate process. Its posterior end (probably the dorsal condyle) is close to the posterior curved end of the squamosal, and the anterior end (probably the ventral condyle) is close to the mandibular condyle. The scan images show that this bone mass bears a narrow anterior end that shows a condylar structure (Appendix 3) and is slightly divided. No further details can be recognized. However, the 'hockey-stick' shape of the squamosal provides strong evidence that the quadrate was streptostylic.

Epipterygoid. A slender columnar epipterygoid (Figs 3; 4A), shown more clearly in the CT scan images (Appendix 3), lies parallel to the quadrate process of the right pterygoid and medial to the squamosal.

Palate. The palate is largely obscured in surface view, but some details are revealed by the CT scans. Within the right naris, there is a sub-triangular, laminar bone fragment that, by position, could be the septomaxilla or vomer, but by shape is more likely to be the latter (Fig. 3). On the part specimen, a short single row of 4-5 small teeth is revealed lying roughly beneath the left naso-maxillary suture (Fig. 7; Appendix 3), and anterior to the right prefrontal, with a similar but shorter row running roughly parallel to it on the left side. Given their position, these must be palatine teeth and their separation suggests the interpterygoid vacuity probably extended forward between the palatines. The right pterygoid is visible on the surface (Fig. 3), but is seen more clearly in the scan of the part block (Fig. 7; Appendix 3). It is Y-shaped, with a lamina between the palatine ramus and the pterygoid flange. The palatal plate is partially obscured within the orbit, but a row of three teeth can be seen on the CT scans, marking the medial edge of the palatine ramus (Fig. 7). The quadrate process is moderately long, and terminates medial to the quadrate. The left pterygoid is only partially visible (the base of the quadrate process is just visible on the surface), but a J-shaped patch of teeth, in which the medial arm of the 'J' is longer than the lateral one, can be seen on the CT scans. In both cases, the pterygoid teeth appear larger than the palatine ones.

The right ectopterygoid articulates with the dorsal surface of the pterygoid flange from anterior to posterior, and then extends almost directly anteriorly to meet the maxilla in the anterior margin of the orbit. The bone also meets the jugal.

Braincase. The braincase was relatively large and was probably originally exposed behind the short parietal table. It is

Downloaded From: https://bioone.org/journals/Geodiversitas on 18 Nov 2019
Terms of Use: https://bioone.org/terms-of-use Access provided by University College London

FIG. 6. — *Hongshanxi xiei* n. gen., n. sp., pelvis, hind limb, and tail: **A**, hind limbs and pelvis, main block; **B**, tail, main block. Abbreviations: **ac.L**, left astragalocalcaneum; **ac.R**, right astragalocalcaneum; **as**, autotomy septum; **cav1**-**cav20**, caudal vertebrae; **d1**-**d5**, digits 1-5; **dt4**, distal tarsal 4; **fe.L**, left femur; **fe.R**, right femur; **fi.L**, left fibula; **fi.R**, right fibula; **il.R**, right ilium; **is.R**, right ischium; **mt5**, fifth metatarsal; **pu.L**, left pubis; **sv1**-**sv2**, sacral vertebrae 1-2; **ti.L**, left tibia; **ti.R**, right tibia. The long square bracket in **B** indicates the regenerated part of the tail. Scale bar: 5 mm

badly crushed and difficult to interpret in surface view, but the CT scan images of the main block (Fig. 7; Appendix 3) reveal the outlines of the basal elements. The sphenoid bears basipterygoid processes that diverge from one another at an angle of around 60°. They are of medium length and widen slightly towards their tips. The parasphenoid (Fig. 3A) is slender and tapers to a tip that is preserved posterior to the right posterior process of the frontal, exposed due to the

Downloaded From: https://bioone.org/journals/Geodiversitas on 18 Nov 2019
Terms of Use: https://bioone.org/terms-of-use Access provided by University College London

loss of the right half of the parietal. The lateral margins of the basisphenoid are fairly straight and the bone expands smoothly towards the suture with the basioccipital. This is the widest part of the basal plate and bears the basal tubera. Behind this point, the basioccipital narrows posteriorly into the condylar region. As a result the whole plate, in outline, forms a rhomboid with the small basal tubera at the lateral apices of the plate and the tripartite occipital condyle posteriorly. The posterior braincase floor is exposed in dorsal view at the surface (Figs 3A; 4A), showing the paired exoccipitals, perforated by hypoglossal foramina, meeting a posteriorly tapering central basioccipital. Little can be discerned of the dorsal braincase components, other than a bone mass to each side of the occipital region that must represent the otic capsules. On the right side, this bone mass extends posterolaterally into what is probably a paroccipital process.

Lower jaw

The left lower jaw lies under the skull and is visible only where it has been pushed through the dorsal surface (Fig. 3A). The right mandible lies adjacent to the right maxilla, but is split between the two blocks (Fig. 3). As a result, very little detail is visible at the surface, although the CT scans provide further information. The left dentary is shallow and tapers anteriorly, with a straight ventral margin. Labially, the bone is perforated by 7-8 neurovascular foramina of roughly equal size (Appendix 3). Lingually, the subdental ridge is shallow with little evident subdental gutter. The Meckelian fossa is also shallow and the presence or absence of a splenial cannot be determined. The teeth are similar to those on the maxilla, with a pleurodont implantation. The left dentary bears 17 tooth positions of which 12 are filled with mature teeth, and the right dentary (counterpart block) has 16-17 tooth positions, of which 11 are filled. The postdentary bones are preserved on both sides but are damaged. The left coronoid is exposed on the main block and the CT scan images show it as a prominent process with a narrow, slightly posteriorly recurved apex and a plate-like medial surface (Fig. 7). On the right side of the scan, the surangular and prearticular are visible as outlines culminating at the posterior articular region. The surangular has horizontal dorsal margin and there seems to be a short retroarticular process.

Hyoid

Long slender ceratobranchial elements are visible on both sides on the surface (Fig. 3) and in the CT scan images (Fig. 7; Appendix 3) of the main block.

Axial skeleton (Figs 2; 5; 6)

The vertebral column is rather crushed, especially in the cervical region, making an accurate description and count difficult. Most of the vertebrae are preserved in an oblique dorsolateral view (Fig. 6A) in which the neural arch and pedicle lie on the same plane and the centrum is obscured. As far as can be determined, these centra are procoelous but the posterior condyles are small and may be incompletely ossified. The neural spines appear to be little developed.

On the main block a small rounded structure immediately posterior to the occiput is likely to be the dens of the axis (Fig. 3A), with the remainder of the atlas and axis within the bone mass posterior to the parietal. A short gap separates these two vertebrae from the main group of cervical vertebrae comprising three vertebrae bearing short ribs and a further two with longer ribs that did not meet the sternum (as indicated by preserved ventral cartilages). This gives a minimum count of seven cervicals. However, the counterpart block bears a partial centrum that fits the gap between the axis and the first rib bearing cervical, making a total of eight cervicals, with the first rib borne on the fourth cervical. The last cervical is followed by a series of anterior dorsal vertebrae, of which at least five preserve cartilaginous extensions that curve inward to meet the cartilaginous sternum, of which most is obscured (Fig. 5A). A further 13 dorsal vertebrae follow the sternal series, giving a dorsal count of 18 and a total presacral count of 26. Following the two sacral vertebrae, 19 caudals are preserved, of which the anterior elements bear long, laterally directed transverse processes (Fig. 6A) that gradually decrease in size and are then lost. The loss of the transverse process coincides roughly with the appearance of the autotomy septum (Fig. 6B), making it difficult to determine the relationship between the transverse process and septum, but the septum appears to be positioned roughly mid-centrum on each vertebra. Following the nineteenth caudal, the tail continues as a cartilage replacement (Fig. 6B) for a length roughly similar to that of the remaining tail. However, the tail is then obscured by matrix so it may originally have been longer. The ribs are single headed and are present as free (i.e. unfused) elements on all dorsal vertebrae.

Forelimb and pectoral girdle

The scapulocoracoids are split between the two blocks. The scapula is longer than wide and is expanded along its dorsal margin. The coracoid is large, but it is not clear whether either scapula or coracoid is fenestrated. Dorsal to the right scapula, there is a calcified lamina that might be the suprascapula. The interclavicle is obscured, but the clavicles are visible (Fig. 5A, B) as curved blades that gradually widen medially but are not abruptly expanded or fenestrate. A cartilage sternum is present but only the margins are visible to either side of the vertebral column, with two of the anterior sternal ribs in contact.

Both forelimbs are present, the left being the better preserved (Fig. 5C). They are conspicuous in the size of the manus which is longer than the humerus and forelimb combined (humerus 8 mm; radius/ulna 5.8 mm; manus 14.4 mm). The humerus has a thick, untwisted shaft. The proximal head is slightly expanded, but lacks a strong deltopectoral crest (although allowance should be made for the immaturity of the specimen). The proximal epiphysis is ossified (on both sides), but is not fused with the humeral body. The distal head is also unexpanded, and the radial and ulna condyles

Downloaded From: https://bioone.org/journals/Geodiversitas on 18 Nov 2019
Terms of Use: https://bioone.org/terms-of-use Access provided by University College London

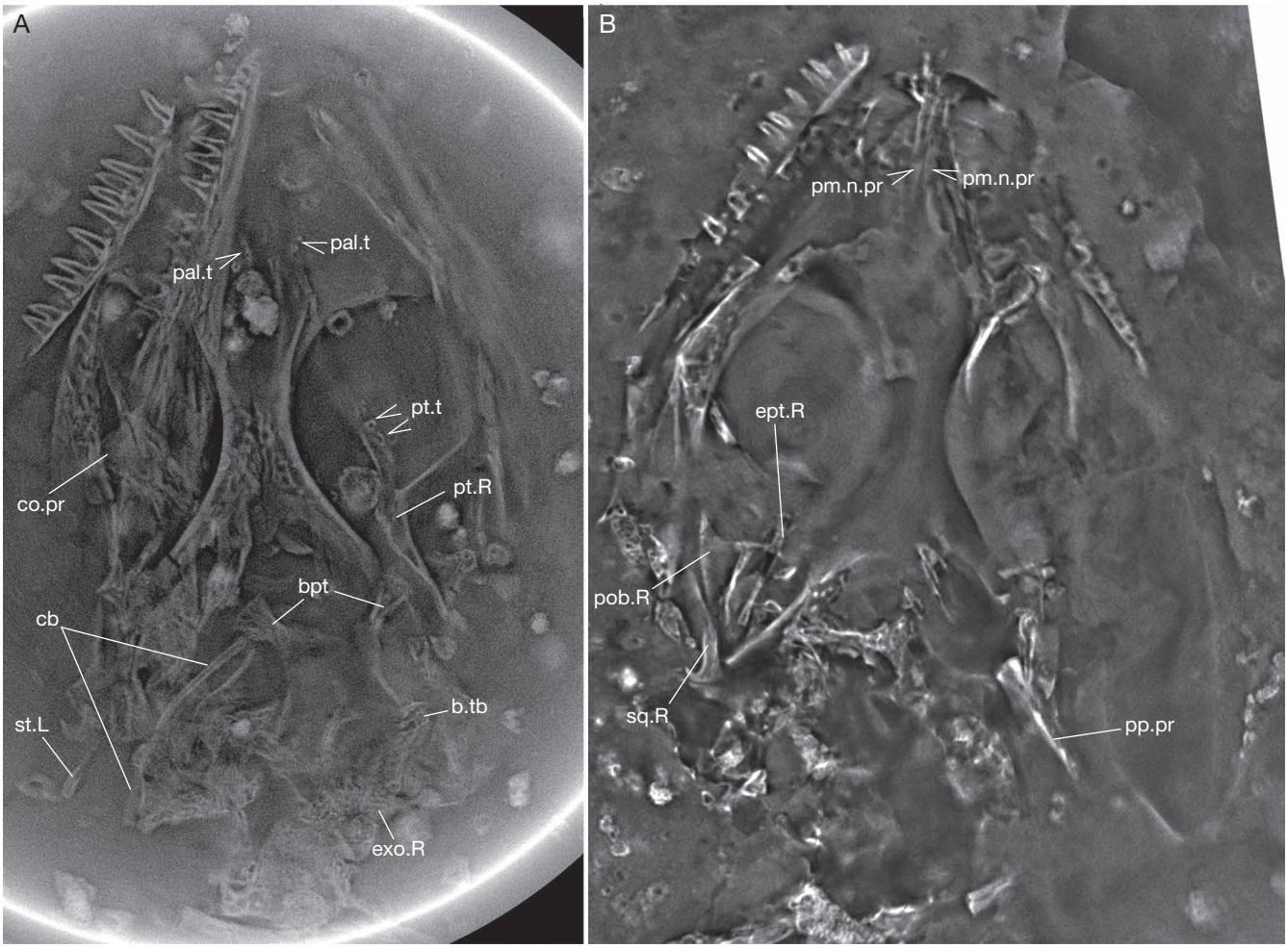

FIG. 7. — *Hongshanxi xiei* n. gen., n. sp., additional cranial features from CL scan images of the part block (**A**) and the counterpart block (**B**). Abbreviations: **bpt**, basipterygoid process; **b.tb**, basal tubercle; **cb**, ceratobranchial; **co.pr**, coronoid process; **ept.R**, right epipterygoid; **exo.R**, right exoccipital/opisthotic; **pal.t**, palatine teeth; **pm.n.pr**, nasal process of premaxilla; **pob.R**, right postorbital; **pp.pr**, postparietal process; **pt.R**, right pterygoid; **pt.t**, pterygoid teeth; **sq.R**, right squamosal; **st.L**, left supratemporal.

are not ossified. The radius and ulna are of similar width with no conspicuous features. The proximal and distal epiphyses of the radius were still unmineralized. The ulna olecranon is ossified, but is not attached to the shaft. The carpus is ossified with finished surfaces on the individual elements. However, the bones are crushed together making it difficult to get an accurate description. The radiale and ulnare can be identified, as well as a pisiform. In the distal row, there is a large distal carpal 4 and, apparently, no distal carpal five, but the centralia and medial distal elements are too crushed. The hand has a phalangeal formula of 2:3:4:5:3. The phalanges are all of similar length and the unguals are sharp and slightly curved. The ungual on the first digit is somewhat larger than the others.

Hind limb and pelvis

The bones of the pelvis are well-formed but not co-ossified (Fig. 6A). The ilium has a slender blade that appears to have been horizontal or slightly inclined in orientation. There is no anterior tubercle. The pubis is also quite narrow. The blade is directed anteromedially, but more medial than anterior. It tapers towards its distal end, although the tip is hidden below the vertebral column. There is very little development of a pectineal tubercle, just a slight swelling of the anterior margin a little less than half the distance from the acetabulum to the symphysis. The ischium is quadrangular with a small posterior tubercle.

Like the humerus, the femur (13.3 mm) is only slightly expanded proximally and there is no development of the greater trochanter (Fig. 6A). The shaft is of similar width throughout, with a slight curvature towards the distal end. The proximal epiphysis is ossified, and not fused with the shaft, but the distal one is undeveloped. The tibia (9.2 mm) is also robust, with a slight inward curvature. The epiphyses are not ossified making it impossible to determine whether there was a distal notch. The fibula is of similar length and without distinguishing features. The articular surface for the astragalocalcaneum completely covers its distal end. The astragalocalcanum itself is proximodistally short and wide. The astragalus and calcaneum are sutured immov-

Downloaded From: https://bioone.org/journals/Geodiversitas on 18 Nov 2019
Terms of Use: https://bioone.org/terms-of-use Access provided by University College London

ably, but the suture line is just visible. The calcaneum has a lateral flange rather than a tuberosity. Tibial and fibular facets are well separated. Distally, there is a large distal tarsal (DT) four and a smaller DT three. The foot is long (24 mm), with phalanges of similar length to one another, although the proximal phalanx of digit 4 is almost as long as the metatarsal of that digit. There is no elongation of the penultimate phalanges and the unguals are sharp and slightly recurved. The angle of the fifth digit indicates that the fifth metatarsal is hooked, but the bones are damaged and do not reveal details of the plantar tubercles. The phalangeal formula is 2:3:4:5:4.

Soft tissue

The body outline is visible as a light stain on the dark surface of the matrix. The outline of the body and limbs is not exceptional, but the tail decreases sharply in diameter at the commencement of the replacement region. Individual scales are visible only in patches, notably on the torso of the counterpart block (square to rhomboid ventral scales) and in the cheek region overlying one of the patches of large osteoderms. Here the scales are seen to be very small and overlapping (dorsal scales).

The body does not have a covering of osteoderms, but there are scattered small patches of white material within the body outline (e.g. Fig. 5A, small asterisks) suggesting there may have been a diffuse arrangement of mineralizations, perhaps associated with skin tubercles.

PHYLOGENETIC ANALYSIS

Data and methods

We coded *Hongshanxi* n. gen. into the data matrix of Gauthier *et al.* (2012) which has 610 characters and 192 taxa. However, as published this matrix contains very few of the Early Cretaceous fossil lizards that have been described in the literature. We therefore added the following well-preserved Early Cretaceous genera to the matrix (based on our own work on these taxa): the Chinese *Yabeinosaurus* (Evans *et al.* 2005; Evans & Wang 2012), *Dalinghosaurus* (Evans & Wang 2005; Evans *et al.* 2007), *Liushusaurus* (Evans & Wang 2010); the Japanese *Sakurasaurus* Evans & Manabe, 1999 (Evans & Manabe 1999, 2009); the Early Cretaceous Spanish *Jucaraseps* Bolet & Evans, 2012 (Bolet & Evans 2012), *Hoyalacerta* Evans & Barbadillo, 1999 (Evans & Barbadillo 1999), *Meyasaurus* Vidal, 1915 (Evans & Barbadillo 1997), and *Scandensia* Evans & Barbadillo, 1998 (Evans & Barbadillo 1998, Bolet & Evans 2011); and the Early Cretaceous Italian *Chometokadmon* Costa, 1864 (Evans *et al.* 2006).

Phylogenetic analyses based on both molecular and combined evidence (molecular+morphological) consistently find a tree topology that differs from that of traditional morphological analyses (e.g. Townsend *et al.* 2004; Wiens *et al.* 2010; Pyron *et al.* 2013; Reeder *et al.* 2015; Zheng & Wiens 2016; Streicher & Wiens 2017). We therefore constructed a backbone constraint tree based on the molecular data with gekkotans and/or dibamids placed as the sister group to a clade in which first scincoids and then lacertoids (including amphisbaenians) are placed as successive outgroups to Toxicofera, comprising anguimorphs, snakes, and iguanians. Fourteen constraints were imposed at the following nodes: 1) Lepidosauria; 2) Squamata; 3) non-gekkotan/non-dibamid clade; 4) Gekkota; 5) Scincoidea; 6) Scincidae+Cordyliformes; 7) non-scincoid squamates; 8) Lacertoidea; 9) Lacertidae+Amphisbaenia; 10) Iguania +Anguimorpha+Serpentes; 11) Iguania; 12) Anguimorpha; 13) Serpentes; 14) Iguania+Anguimorpha (reflecting Streicher & Wiens 2017). The taxa used to build the constraint tree were *Gephyrosaurus* Evans, 1980, *Dibamus* Duméril & Bibron, 1839, *Gekko* Laurenti, 1768, *Delma* Gray, 1831, *Xantusia* Baird, 1858, *Scincus* Laurenti, 1768, *Cordylus* Laurenti, 1768, *Tupinambis* Daudin, 1802, *Lacerta* Linnaeus, 1758, *Rhineura* Cope, 1861, *Anolis* Daudin, 1802, *Physignathus* Cuvier, 1829, *Xenosaurus* Peters, 1861, *Lanthanotus* Steindachner, 1878, *Cylindrophis* Wagler, 1928, and *Python* Daudin, 1803. All other taxa, living and fossil, were designated as floaters.

Two further analyses were conducted with a smaller extant squamate data set, as used by Koch & Gauthier (2018), that omitted the non-snake serpentiform squamate taxa (e.g. notably Dibamidae, Amphisbaenia) which frequently group convergently in morphology-based analyses. The nine Early Cretaceous taxa were also included (total 56 taxa). The constrained analysis used a taxon group that is consistent with the data set of Koch & Gauthier (2018), of *Sphenodon* Gray, 1831, *Eublepharis* Gray, 1827, *Saltuarius* Couper, Covacevich & Moritz, 1993, *Tiliqua* Gray, 1825, *Cordylosaurus* Gray, 1865, *Pholidobolus* Peters, 1863, *Lacerta*, *Cylindrophis*, *Varanus* Merrem, 1820, *Uromastyx* Merrem, 1820, and other taxa as floaters.

The analyses were run in TNT v 1.5 (Goloboff & Catalano 2016), with and without constraints, and with the characters set as unordered or ordered as in Gauthier *et al.* (2012). The analyses with the full data set used the New Technology search with Ratchet (20 iterations), and 1000 replicates in RAM (default parameters for other variables). We chose the Early Jurassic rhynchocephalian *Gephyrosaurus* rather than the more derived living taxon, *Sphenodon* (as used by Gauthier *et al.* 2012) as TNT allows only one designated outgroup. The last two runs with the smaller data set were conducted using the traditional search option (TBR).

Results

Although the tree topology differed between analyses for many individual taxa, *Hongshanxi* n. gen. was consistently placed in one of two positions, depending on whether or not a backbone molecular constraint tree was used (Fig. 8; Appendices 1, 2). With minor differences, the unconstrained analyses placed *Hongshanxi* n. gen. into a variably resolved position on the stem of a traditional Scleroglossa (Gekkota, Anguimorpha, Lacertoidea, Scin-

Downloaded From: https://bioone.org/journals/Geodiversitas on 18 Nov 2019
Terms of Use: https://bioone.org/terms-of-use Access provided by University College London

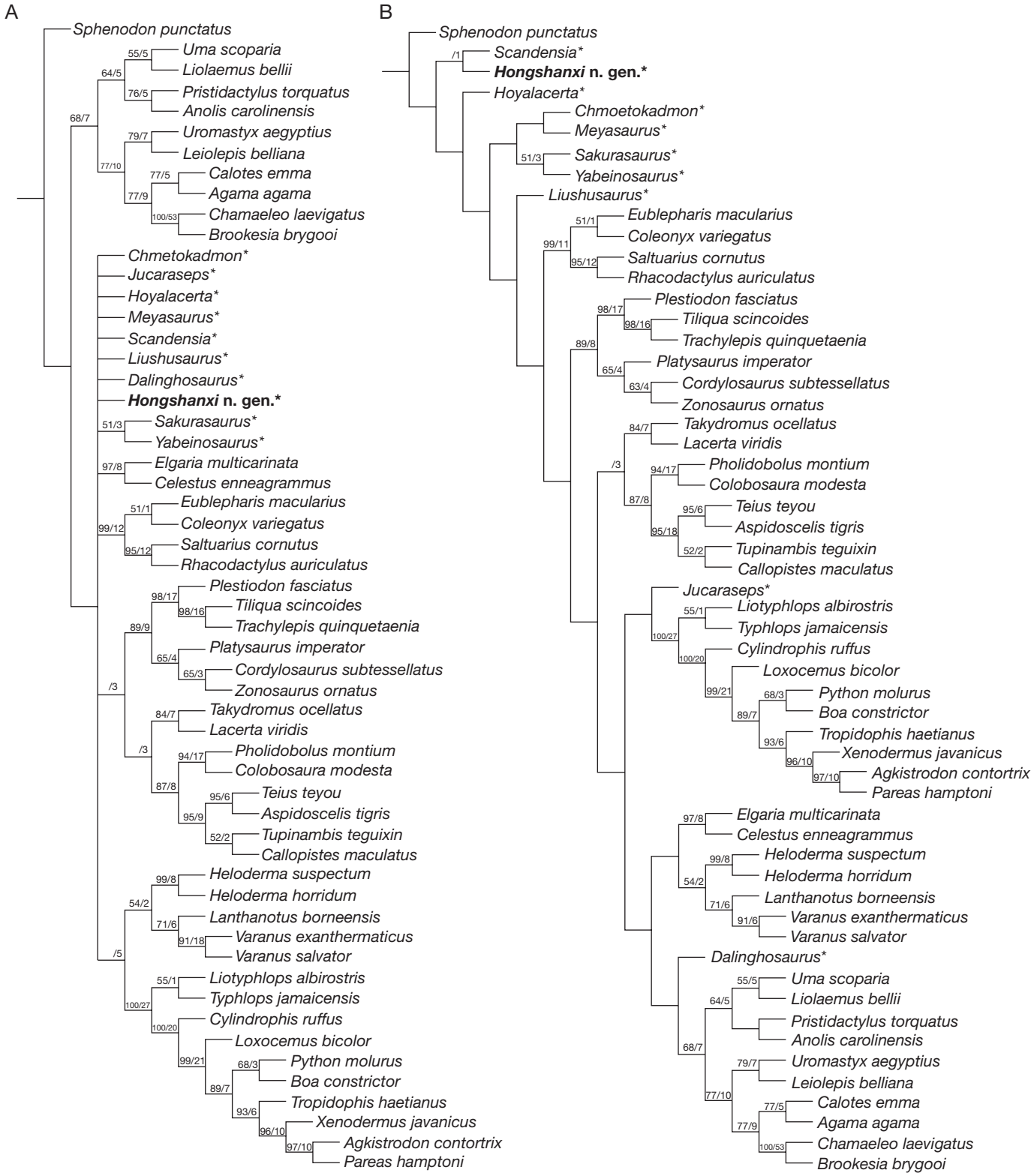

FIG. 8. — Phylogenetic position of *Hongshanxi xiei* n. gen., n. sp.: **A**, ordered characters without molecular constraints; **B**, ordered characters with molecular constraints.

coidea, Serpentes) (Fig. 8A). The analyses run with the backbone molecular constraint tree placed *Hongshanxi* n. gen. on the squamate stem, frequently in a sister group relationship with the Early Cretaceous Spanish lizard *Scandensia* (but see Discussion) (Fig. 8B). Thus the position of *Hongshanxi* n. gen. (and many of the other Jurassic/Early Cretaceous taxa) seems to be strongly influenced by the position of Gekkota.

Downloaded From: https://bioone.org/journals/Geodiversitas on 18 Nov 2019
Terms of Use: https://bioone.org/terms-of-use Access provided by University College London

DISCUSSION

Phylogenetic analysis

The structure of the temporal region (notably the 'hockey-stick' squamosal shape) and features of the postcranial skeleton, including the procoelous vertebrae and gracile pelvis, indicate that *Hongshanxi* n. gen. is a squamate. However, as with many other Jurassic and early Cretaceous taxa (e.g. *Scandensia, Yabeinosaurus, Hoyalacerta, Liushusaurus*), the phylogenetic position of *Hongshanxi* n. gen. cannot be clearly resolved. A purely morphological analysis places it as a stem-scleroglossan (sensu Gauthier *et al.* 2012), but all previous molecular and combined analyses have rejected the concept of Scleroglossa as they place Gekkota (with or without Dibamidae) as the sister group of all other crown squamates. The only morphology based analysis to place Gekkota as the sister group of other squamates was that of Simões *et al.* (2018), but their phylogeny is controversial in other ways, notably the inclusion of some stem-lepidosaurs (e.g. *Marmoretta*) within Squamata. If the molecular tree is a correct representation of living squamate relationships, and we accept that it is, then there are fundamental flaws in the way that we are identifying and defining morphological characters. Moreover, many Jurassic/Early Cretaceous fossil lizard taxa – though relatively derived in some aspects of their morphology – frequently lack (whether through incompleteness or plesiomorphy) the 'key' morphological characters that might associate them unambiguously with a crown-clade. Fossil taxa therefore tend a) to be drawn stemwards; b) to act as unstable rogue taxa, moving around the tree and reducing its resolution; or c) to cluster with other fossil taxa on the basis of character states inferred by the computer program but, in reality, unknown.

Comparison with contemporaneous taxa

The combination of characters shown by *Hongshanxi* n. gen., especially the unusual fronto-parietal anatomy and the temporal osteoderms, distinguishes it clearly from any of the Jurassic-Early Cretaceous Chinese or Japanese (e.g. Evans & Matsumoto 2015) lizards, as far as they are known, and from the majority of contemporaneous lizards from other localities. The only fossil lizard that shows a somewhat similar fronto-parietal morphology is *Hoyalacerta sanzi* from the Early Cretaceous Spanish locality of Las Hoyas (Evans & Barbadillo 1999). Here, again, the frontals (paired unlike *Hongshanxi* n. gen.) have long posterolateral processes that seem to fit into anterolateral recesses in the parietal. Unfortunately, the temporal region is poorly preserved in *Hoyalacerta*, limiting comparison. *Hoyalacerta*, like *Hongshanxi* n. gen., has a slender mandible but unlike *Hongshanxi* n. gen. has around 40 small teeth along each tooth row and there is no trace of cranial osteoderms. The postcranial proportions are also quite different as *Hoyalacerta* has limbs that are short relative to the length of the vertebral column.

In some of the analyses, *Hongshanxi* n. gen. was placed as the sister taxon of the Spanish Early Cretaceous *Scandensia* (Evans & Barbadillo 1998), but this appears to be an artefact of shared primitive states and missing data (and thus program-estimated character states). When characters are mapped, the only derived character definitely shared by *Scandensia* and *Hongshanxi* n. gen. is Gauthier *et al.* (2012) character 36, fused frontals, a trait found across different clades of squamates and some fossil rhynchocephalians (e.g. *Gephyrosaurus*). The skull of *Scandensia* is very poorly preserved and thus provides little basis for comparison. Moreover, the two genera do not share any significant postcranial features. In contrast to *Hongshanxi* n. gen., *Scandensia* has exceptionally elongate penultimate phalanges, large overlapping body (but not cranial) osteoderms (Bolet & Evans 2011), and a rhomboid interclavicle. *Scandensia* is also considerably smaller than *Hongshanxi* n. gen., with the two known specimens having snout-pelvis lengths of 25 mm and 32-35 mm, in contrast to 55 mm for *Hongshanxi* n. gen.

Three other Jurassic lizards have been described from China, two from Daohugou (possibly contemporaneous with Guancaishan, Callovian-Oxfordian: Evans & Wang 2007, 2009) and one from Shishugou in Xinjiang Uygur Autonomous Region (Oxfordian: Conrad *et al.* 2013). A manuscript on the latter specimen is currently in review/revision but, as reported in the original abstract (Conrad *et al.* 2013), the new Shishugou taxon differs from *Hongshanxi* n. gen. in having a complete covering of osteoderms, cusps on the teeth, and an unspecialised frontal. The two Daohugou lizards are less mature skeletally than *Hongshanxi* n. gen. and neither has been named due to the poor preservation. One (SPL 43.7 mm, Evans & Wang 2007) is represented by scale traces and skeletal impressions. Like *Hongshanxi* n. gen., it has a long hand, but the forelimb as a whole is short in relation to snout-pelvis length (SPL) (38.2 vs 51.3% in *Hongshanxi* n. gen.), as is the hind limb (57.2 vs 84.5% in *Hongshanxi* n. gen.). Even allowing for ontogenetic differences, body proportions clearly separate these two morphotypes. The second Daohugou lizard (Evans & Wang 2009) is larger (SPL 60.1mm) than the first (or *Hongshanxi* n. gen.). Like *Hongshanxi* n. gen., it has large hand (20.8% SPL vs 26.2% in *Hongshanxi* n. gen.), but the foot is proportionally shorter (28% SPL vs 43.6%). The skull is difficult to compare with that of *Hongshanxi* n. gen. but, as preserved, differs in frontal shape and length (shorter in the Daohugou lizard), parietal length (longer in the Daohugou lizard), and length of the penultimate phalanges (longer in the Daohugou lizard). We are therefore confident that *Hongshanxi* n. gen. is generically distinct from previously described taxa, but its phylogenetic position remains uncertain pending new analyses and the addition of further fossil taxa.

Lifestyle

Osteoderms are generally considered to function as protective armour, but where their distribution is limited to parts of the head, they are something of an enigma. Free (i.e. not bonded to bone) temporal and supraocular osteoderms are a feature of some larger extant lacertid lizards (e.g. Arnold

Downloaded From: https://bioone.org/journals/Geodiversitas on 18 Nov 2019
Terms of Use: https://bioone.org/terms-of-use Access provided by University College London

et al. 2007; SEE unpublished work in progress), but the function of these structures remains uncertain. They would seem to be of limited use as an anti-predator device given that the rest of the body is unprotected. However, these large lizards often bite one another forcibly across the head and neck during fights (for territory or females), leaving large surface wounds (Mateo 2015). The temporal osteoderms might, plausibly, help to limit deeper injuries, or they may help to strengthen the skull in biting. In *Hongshanxi* n. gen., the relatively low number of sharp, well-spaced teeth suggests a diet of large insects, as smaller prey items would typically be caught with the tongue, and the absence of cusps renders a herbivorous or omnivorous diet unlikely (e.g. Hotton 1955; Herrel *et al.* 2004). The deep maxilla, fused nasals, and extended frontal, in conjunction with the temporal osteoderms, may all have helped to strengthen the skull during feeding. The large manus and pes of *Hongshanxi* n. gen., coupled with relatively long limbs, suggest it may have climbed or scrambled on uneven surfaces.

Acknowledgements
We thank Wei Gao and Pengfei Yin (IVPP) for photographing the specimens and assisting with the Micro-Computed Laminography scans, respectively. We also would like to thank Dr Maridet Olivier (JURASSICA Museum, Switzerland) for the help with the French abstract. This work was supported by the National Natural Science Foundation of China (41688103) and the Strategic Priority Research Program (B) of the Chinese Academy of Sciences (XDB18000000, XDB26000000). The CAS President's International Fellowship Initiative (PIFI) awarded to SEE in 2016 supported her visit to IVPP, CAS, during which this work started. We record our thanks to the Willi Hennig Society for free access to the phylogenetics program TNT v1.5. Our thanks also go to Marc Augé and Sebastiàn Apesteguìa and the editors for their helpful comments on an earlier version of the manuscript.

REFERENCES

ARNOLD E. N., ARRIBAS O. & CARRANZA S. 2007. — Systematics of the Palaearctic and Oriental lizard tribe Lacertini (Squamata: Lacertidae: Lacertinae). *Zootaxa* 1430: 1-86. https://doi.org/10.11646/zootaxa.1430.1.1

BOLET A. & EVANS S. E. 2011. — New material of the enigmatic *Scandensia*, an Early Cretaceous lizard from the Iberian Peninsula. *Special Papers in Palaeontology* 86: 99-108.

BOLET A. & EVANS S. E. 2012. — A tiny lizard (Lepidosauria, Squamata) from the Lower Cretaceous of Spain. *Palaeontology* 55: 491-500. https://doi.org/10.1111/j.1475-4983.2012.01145.x

CONRAD J. L., WANG Y., XU X., PYRON A. & CLARK J. 2013. — Skeleton of a heavily armored and long legged Middle Jurassic lizard (Squamata, Reptilia). *Supplement to the online Journal of Vertebrate Paleontology, 73rd Annual Meeting, Abstracts*: 108.

DONG L.-P., WANG Y. & EVANS S. E. 2017. — A new lizard (Reptilia: Squamata) from the Early Cretaceous Yixian Formation of China, with a taxonomic revision of *Yabeinosaurus*. *Cretaceous Research* 72: 161-171. https://doi.org/10.1016/j.cretres.2016.12.017

DONG L.-P., XU X., WANG Y. & EVANS S. E. 2018. — The lizard genera *Bainguis* and *Parmeosaurus* from the Upper Cretaceous of China and Mongolia. *Cretaceous Research* 85: 95-108. https://doi.org/10.1016/j.cretres.2018.01.002

ENDO R. & SHIKAMA T. 1942. — Mesozoic reptilian fauna in the Jehol mountainland, Manchoukuo. *Bulletin of the Central National Museum of Manchoukuo* 3: 1-19.

ESTES R. 1983. — *Sauria Terrestria, Amphisbaenia*, *in* Handbuch der Paläoherpetologie – Encyclopedia of Paleoherpetology. Part 10A. Gustav Fischer Verlag, Stuttgart, New York: 1-245

ESTES R., DE QUEIROZ K. & GAUTHIER J. 1988. — Phylogenetic relationships within Squamata, *in* ESTES R. & PREGILL G. (eds), *Phylogenetic Relationships of the Lizard Families*. Stanford University Press, Stanford: 119-281. http://hdl.handle.net/10088/6457

EVANS S. E. & BARBADILLO L. J. 1997. — Early Cretaceous lizards from Las Hoyas, Spain. *Zoological Journal of Linnean Society* 119: 1-27. https://doi.org/10.1111/j.1096-3642.1997.tb00134.x

EVANS S. E. & BARBADILLO L. J. 1998. — An unusual lizard (Reptilia, Squamata) from the Early Cretaceous of Las Hoyas, Spain. *Zoological Journal of Linnean Society* 124: 235-266. https://doi.org/10.1111/j.1096-3642.1998.tb00576.x

EVANS S. E. & BARBADILLO L. J. 1999. — A short-limbed lizard from the Lower Cretaceous of Spain. *Special Papers in Palaeontology* 60: 73-85.

EVANS S. E. & MANABE M. 1999. — Early Cretaceous lizards from the Okurodani Formation of Japan. *Geobios* 32: 889-899. https://doi.org/10.1016/S0016-6995(99)80871-7

EVANS S. E. & MANABE M. 2009. — The Early Cretaceous lizards of Eastern Asia: new material of *Sakurasaurus* from Japan. *Special Papers in Palaeontology* 81: 43-59.

EVANS S. E. & MATSUMOTO R. 2015. — An assemblage of lizards from the Early Cretaceous of Japan. *Palaeontologica Electronica* 18: 1-36. https://doi.org/10.26879/519

EVANS S. E., RAIA P. & BARBERA C. 2006. — A revision of the Early Cretaceous lizard *Chometokadmon* from Italy. *Cretaceous Research* 27: 673-683. https://doi.org/10.1016/j.cretres.2006.03.004

EVANS S. E. & WANG Y. 2005. —The Early Cretaceous lizard *Dalinghosaurus* from China. *Acta Palaeontologica Polonica* 50: 725-742.

EVANS S. E. & WANG Y. 2007. — A juvenile lizard specimen with well-preserved skin impressions from the Upper Jurassic/Lower Cretaceous of Daohugou, Inner Mongolia, China. *Naturwissenschaften* 94: 431-439. https://doi.org/10.1007/s00114-006-0214-y

EVANS S. E. & WANG Y. 2009. — A long-limbed lizard from the Upper Jurassic/Lower Cretaceous of Daohugou, Ningcheng, Nei Mongol, China. *Vertebrata PalAsiatica* 47 (1): 21-34.

EVANS S. E. & WANG Y. 2010. — A new lizard (Reptilia: Squamata) with exquisite preservation of soft tissue from the Lower Cretaceous of Inner Mongolia, China. *Journal of Systematic Palaeontology* 8: 81-95. https://doi.org/10.1080/14772010903537773

EVANS S. E. & WANG Y. 2012. — New material of the Early Cretaceous lizard *Yabeinosaurus* from China. *Cretaceous Research* 34: 48-60. https://doi.org/10.1016/j.cretres.2011.10.004

EVANS S. E., WANG Y. & JONES M. E. H. 2007. — An aggregation of lizard skeletons from the Lower Cretaceous of China. *Senckenbergiana Lethaea* 87: 109-118. https://doi.org/10.1007/BF03043910

EVANS S. E., WANG Y. & LI C. 2005. — The Early Cretaceous lizard genus *Yabeinosaurus* from China: resolving an enigma. *Journal of Systematic Palaeontology* 3: 319-335. https://doi.org/10.1017/S1477201905001641

GAO K.-Q. & CHENG Z.-W. 1999. — A new lizard from the Lower Cretaceous of Shandong, China. *Journal of Vertebrate Paleontology* 19: 456-465. https://doi.org/10.1080/02724634.1999.10011158

GAO K.-Q. & HOU L.-H. 1995. — Iguanians from the Upper Cretaceous Djadochta Formation, Gobi Desert, China. *Journal of Vertebrate Paleontology* 15: 57-78. https://doi.org/10.1080/02724634.1995.10011207

Downloaded From: https://bioone.org/journals/Geodiversitas on 18 Nov 2019
Terms of Use: https://bioone.org/terms-of-use Access provided by University College London

GAO K.-Q. & HOU L.-H. 1996. — Systematics and taxonomic diversity of squamates from the Upper Cretaceous Djadochta Formation, Bayan Mandahu, Gobi Desert, People's Republic of China. *Canadian Journal of Earth Sciences* 33: 578-598. https://doi.org/10.1139/e96-043

GAO K.-Q. & SHUBIN N. H. 2012. — Late Jurassic salamandroid from Western Liaoning, China. *Proceedings of the National Academy of Sciences of the United States of America* 109: 5767-5772. https://doi.org/10.1073/pnas.1009828109

GAUTHIER J., KEARNEY M., MAISANO J. A., RIEPPEL O. & BEHLKE A. D. B. 2012. — Assembling the squamate Tree of Life: perspectives from the phenotype and the fossil record. *Bulletin of the Peabody Museum of Natural History* 53: 3-308. https://doi.org/10.3374/014.053.0101

GOLOBOFF P. A. & CATALANO S. A. 2016. — TNT version 1.5, including a full implementation of phylogenetic morphometrics. *Cladistics* 32: 221-238. https://doi.org/10.1111/cla.12160

HAN F.-L., WANG Y., SULLIVAN C., WANG Y.-Q., QIN Z.-C. & XU X. 2016. — Chapter 7: The vertebrates, *in* HUANG D. Y. (ed.), *The Daohugou Biota*. Shanghai Scientific and Technical Publishers, Shanghai: 218-251.

HERREL A., VANHOOYDONCK B. & VAN DAMME R. 2004. — Omnivory in lacertid lizards: adaptive evolution or constraint. *Evolutionary Biology* 17: 974-984. https://doi.org/10.1111/j.1420-9101.2004.00758.x

HOTTON N. 1955. — A survey of adaptive relationships of dentition to diet in the North American Iguanidae. *The American Midland Naturalist* 53: 88-114. https://doi.org/10.2307/2422301

HUANG D.-Y., CAI C.-Y., XU X., WANG X.-L., SU W.-T., LIAO H.-Y., JIANG J.-Q. & SHA J.-G. 2016. — Chapter 3: Daohugou fossil beds and Daohugou biota, *in* HUANG D. Y. (ed.), *The Daohugou Biota*. Shanghai Scientific and Technical Publishers, Shanghai: 37-70.

JI Q., LUO Z.-X., YUAN C.-H. & TABRUM A. R. 2006. — A swimming mammaliaform from the Middle Jurassic and ecomorphological diversification of early mammals. *Science* 311: 1123-1127. https://doi.org/10.1126/science.1123026

JI S.-A. 1998. — A new long-tailed lizard from the Upper Jurassic of Liaoning, China, *in* Department of Geology, Peking University (ed.), *Collected Works of International Symposium on Geological Science, Peking University, Beijing, China.* Seismological Press, Beijing: 496-505.

JI S.-A. & JI Q. 2004. — Postcranial anatomy of the Mesozoic *Dalinghosaurus* (Squamata): evidence from a new specimen of Western Liaoning. *Acta Geologica Sinica* 78: 897-906. https://doi.org/10.1111/j.1755-6724.2004.tb00211.x

JI S.-A., LU L.-W. & BO H.-C. 2001. — New material of *Yabeinosaurus tenuis* (Lacertilia). *Land and Resources* 2001: 41-43 (in Chinese).

KOCH N. M. & GAUTHIER J. A. 2018. — Noise and biases in genomic data may underlie radically different hypotheses for the position of Iguania within Squamata. *PLoS ONE* 13 (8): e0202729. https://doi.org/10.1371/journal.pone.0202729

LI J.-L. 1985. — A new lizard from the Late Jurassic of Subei, Gansu. *Vertebrata PalAsiatica* 23: 13-18 (in Chinese with English summary).

LI P.-P., GAO K.-Q., HOU L.-H. & XU X. 2007. — A gliding lizard from the Early Cretaceous of China. *Proceedings of the National Academy of Sciences of the United States of America* 104: 5507-5509. https://doi.org/10.1073/pnas.0609552104

LIU B.-D., WEI Z.-H., WEI C.-F., WANG Y.-F., YUAN L.-L., SHU Y.-F., QUE J.-M., SUN C.-L., WANG Y.-X., SHAO Y.-M., CHAI J.-B. & WEI L. 2015. — An Industrial Computed Laminography Imaging System. *Proceedings of Digital Industrial Radiology and Computed Tomography* (DIR2015): 22-25.

LIU Y.-Q., LIU Y.-X., JI S.-A. & YANG Z.-Q. 2006. — U-Pb zircon age for the Daohugou Biota at Ningcheng of Inner Mongolia and comments on related issues. *Chinese Science Bulletin* 51: 2634-2644. https://doi.org/10.1007/s11434-006-2165-2

LÜ J.-C., JI S.-A., DONG Z.-M. & WU X.-C. 2008. — An Upper Cretaceous lizard with a lower temporal arcade. *Naturwissenschaften* 95: 663-669. https://doi.org/10.1007/s00114-008-0364-1

MATEO J. A. 2015. — Lagarto ocelado – *Timon lepidus*, *in* SALVADOR A. & MARCO A. (eds), *Enciclopedia Virtual de los Vertebrados Españoles*. *Museo Nacional de Ciencias Naturales, Madrid*. http://www.vertebradosibericos.org. Last consultation on 3rd October 2016

MO J.-Y., XU X. & EVANS S. E. 2010. — The evolution of the lepidosaurian lower temporal bar: new perspectives from the Late Cretaceous of South China. *Proceedings of the Royal Society B, Special Volume on Chinese Fossils* 277: 331-336. https://doi.org/10.1098/rspb.2009.0030

MO J.-Y., XU X. & EVANS S. E. 2012. — A large predatory lizard (Platynota, Squamata) from the Late Cretaceous of South China. *Journal of Systematic Palaeontology* 10: 333-339. https://doi.org/10.1080/14772019.2011.588254

PYRON R. A., BURBRINK F. T. & WIENS J. J. 2013. — A phylogeny and revised classification of Squamata, including 4161 species of lizards and snakes. *BMC Evolutionary Biology* 13: 93. http://www.biomedcentral.com/1471-2148/13/93

REEDER T. W., TOWNSEND T. M., MULCAHY D. G., NOONAN B. P., WOOD P. L. JR, SITES J. W. JR & WIENS J. J. 2015. — Integrated analyses resolve conflicts over squamate reptile phylogeny and reveal unexpected placements for fossil taxa. *PLoS ONE* 10: e0118199. https://doi.org/10.1371/journal.pone.0118199

RICHTER A., WINGS O., PFRETZSCHNER H.-U. & MARTIN R. 2010. — Late Jurassic Squamata and possible Choristodera from the Junggar basin, Xinjiang, Northwest China. *Palaeobiodiversity and Palaeoenvironments* 90: 275-282. https://doi.org/10.1007/s12549-010-0037-x

SIMÕES T. R., CALDWELL M. W., TAŁANDA M., BERNARDI M., PALCI A., VERNYGORA O., BERNANDINI F., MANCINI L. & NYDAM R. L. 2018. — The origin of squamates revealed by a Middle Triassic 'lizard' from the Italian Alps. *Nature* 557: 706-709. https://doi.org/10.1038/s41586-018-0093-3

STREICHER J. W. & WIENS J. J. 2017. — Phylogenomic analyses of more than 4000 nuclear loci resolve the origin of snakes among lizard families. *Biology Letters* 13: 20170393. https://doi.org/10.1098/rsbl.2017.0393

SULLIVAN C., WANG Y., HONE D. W. E., WANG Y.-Q., XU X. & ZHANG F.-C. 2014. — The vertebrates of the Jurassic Daohugou Biota of northeastern China. *Journal of Vertebrate Paleontology* 34: 243-280. https://doi.org/10.1080/02724634.2013.787316

TOWNSEND T. M., LARSON A., LOUIS E. & MACEY J. R. 2004. — Molecular phylogenetics of Squamata: the position of snakes, amphisbaenians, and dibamids, and the root of the squamate tree. *Systematic Biology* 53: 735-757. https://doi.org/10.1080/10635150490522340

WANG Y., DONG L.-P. & EVANS S. E. 2016. — Polydactyly and other limb abnormalities in the Jurassic salamander *Chunerpeton* from China. *Palaeobiodiversity and Palaeoenvironment* 96: 49-59. https://doi.org/10.1007/s12549-015-0219-7

WIENS J. J., KUCZYNSKI C. A., TOWNSEND T. M., REEDER T. W., MULCAHY D. G. & SITES J. W. JR 2010. — Combining phylogenomics and fossils in higher-level squamate reptile phylogeny: molecular data change the placement of fossil taxa. *Systematic Biology* 59: 674-688.

WU X.-C., BRINKMAN D. B. & RUSSELL A. P. 1996. — *Sineoamphisbaena hexatabularis*: an amphisbaenian (Diapsida: Squamata) from the Upper Cretaceous redbeds at Bayan Mandahu (Inner Mongolia, People's Republic of China), and comments on the phylogenetic relationships of the Amphisbaenia. *Canadian Journal of Earth Sciences* 33: 541-577. https://doi.org/10.1139/e96-042

XU L., WU X.-C., LÜ J.-C., JIA S.-H., ZHANG J.-M., PU H.-Y. & ZHANG X.-L. 2014. — A new lizard (Lepidosauria: Squamata)

Downloaded From: https://bioone.org/journals/Geodiversitas on 18 Nov 2019
Terms of Use: https://bioone.org/terms-of-use Access provided by University College London

from the Upper Cretaceous of Henan, China. *Acta Geologica Sinica* 88: 1041-1050. https://doi.org/10.1111/1755-6724.12271

YOUNG C. C. 1958. — On a new locality of *Yabeinosaurus tenuis* Endo and Shikama. *Vertebrata PalAsiatica* 2: 151-156.

ZHANG G.-L. 2008. — *Morphological and Ontogenetic Study on a Mesozoic Salamander (*Chunerpeton tianyiensis*) from Northeastern China*. M. S. thesis, Institute of Vertebrate Paleontology and Paleoanthropology, Beijing, China, 61 p.

ZHENG Y. & WIENS J. J. 2016. — Combining phylogenomic and supermatrix approaches, and a time-calibrated phylogeny for squamate reptiles (lizards and snakes) based on 52 genes and 4162 species. *Molecular Phylogenetics and Evolution* 94: 537-547. https://doi.org/10.1016/j.ympev.2015.10.009

ZHOU Z.-H. & WANG Y. 2017. — Vertebrate assemblages of the Jurassic Yanliao Biota and the Early Cretaceous Jehol Biota: Comparisons and implications. *Palaeoworld* 26: 241-252. https://doi.org/10.1016/j.palwor.2017.01.002)

Submitted on 24 January 2019;
accepted on 31 July 2019;
published on 13 September 2019.

Downloaded From: https://bioone.org/journals/Geodiversitas on 18 Nov 2019
Terms of Use: https://bioone.org/terms-of-use Access provided by University College London

APPENDIX 1. — Strict consensus trees obtained from the analyses of the full data matrix, without molecular constraints. Download a larger version (PDF) of this Figure on http://sciencepress.mnhn.fr/sites/default/files/documents/fr/g2019v41a16-2-fig-s1.pdf.

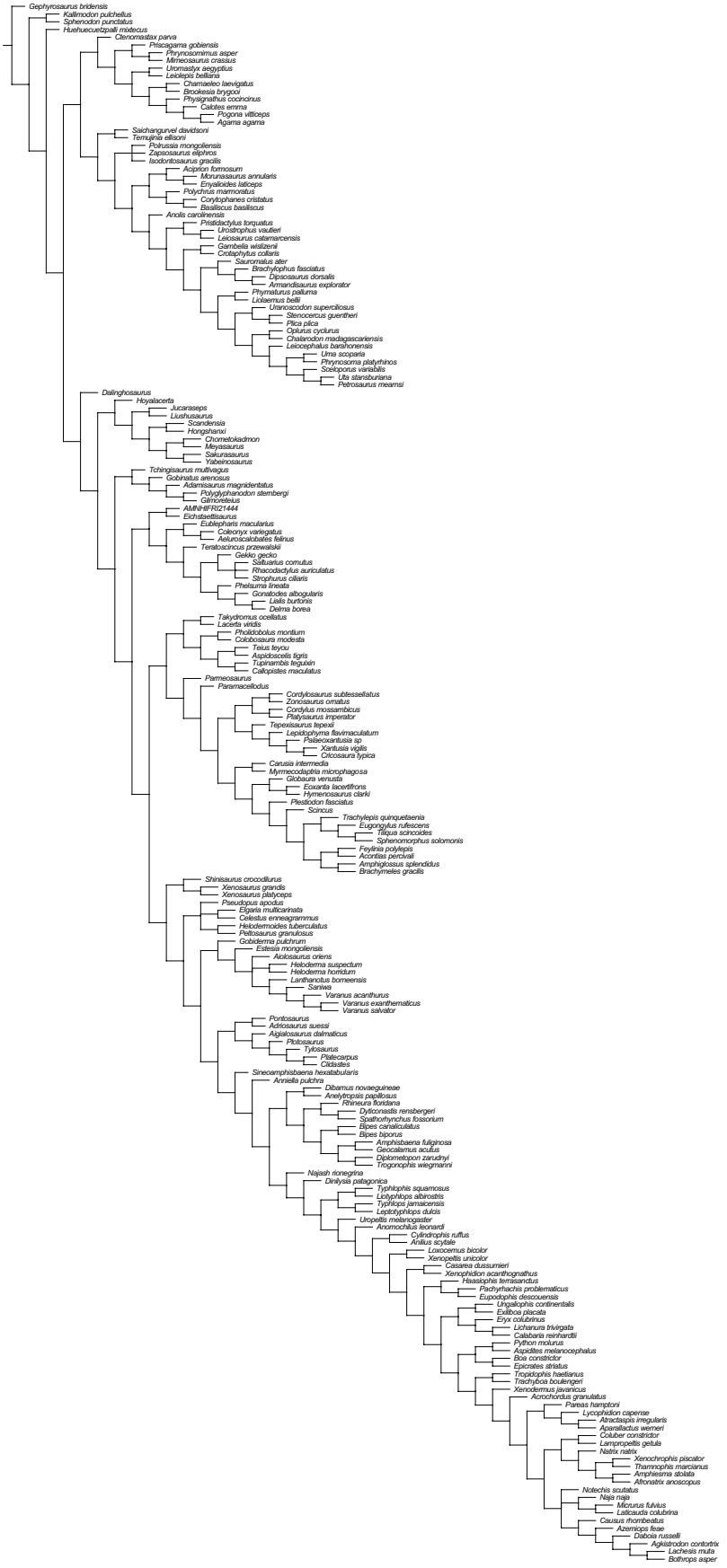

Downloaded From: https://bioone.org/journals/Geodiversitas on 18 Nov 2019
Terms of Use: https://bioone.org/terms-of-use Access provided by University College London

APPENDIX 2. — Strict consensus trees obtained from the analyses of the full data matrix, with molecular constraints. Download a larger version (PDF) of this Figure on http://sciencepress.mnhn.fr/sites/default/files/documents/fr/g2019v41a16-3-fig-s2.pdf.

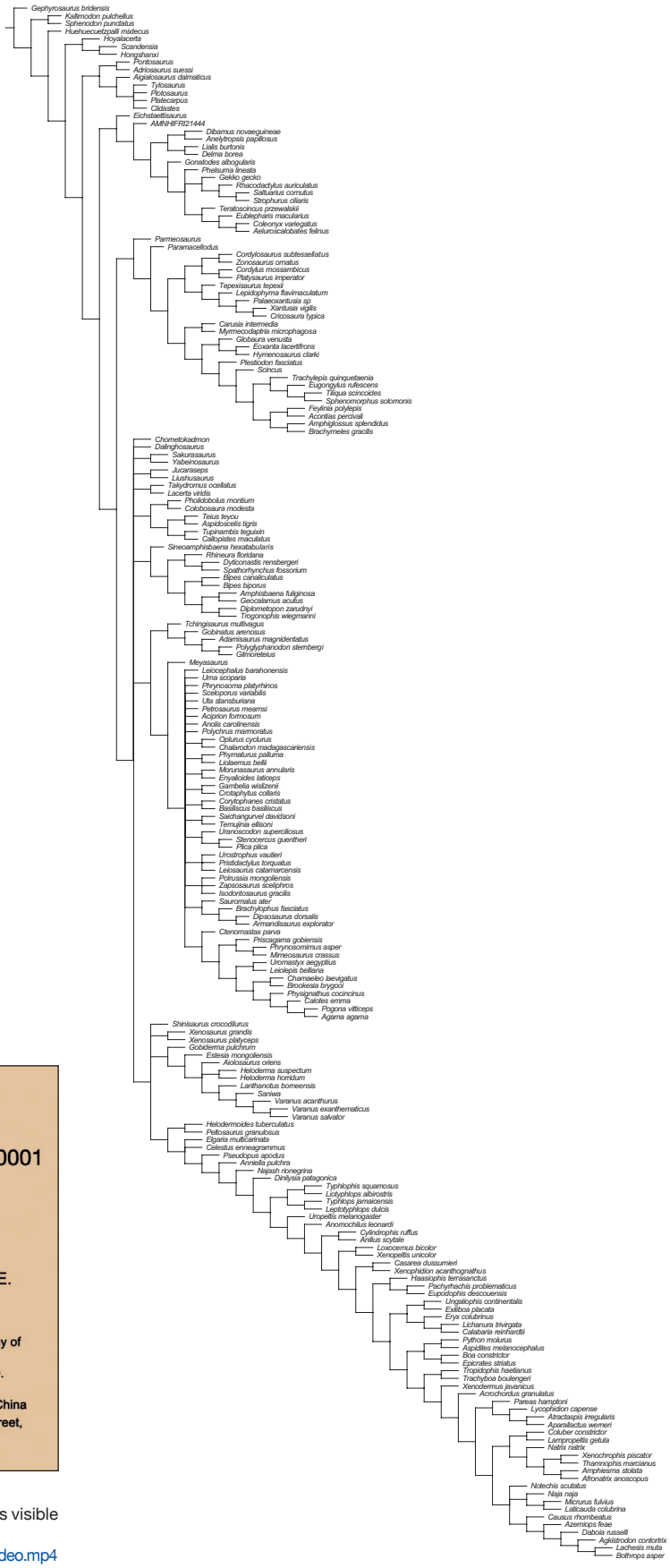

Hongshanxi xiei

CL scan on Jianping County Museum HS-0001

Supplementary information for

A new Jurassic lizard from China

Liping Dong[1,2], Yuan Wang[1,2], Lijie Mou[2], Guoze Zhang[2], Susan E. Evans[3]

[1]Key Laboratory of Vertebrate Evolution and Human Origin of Chinese Academy of Science, Institute of Vertebrate Paleontology and Paleoanthropology, Chinese Academy of Sciences, 142 Xi-Zhi-Men-Wai St, P.O. Box 643, Beijing 100044, China

[2]CAS Center for Excellence in Life and Paleoenvironment, 142 Xi-Zhi-Men-Wai St, P.O. Box 643, Beijing 100044, China

[3]Fossil Protection Office, Jianping Bureau of Land and Resources, Jianping, 122400, China

[4]Department of Cell and Developmental Biology, University College London, Gower Street, London, WC1E 6BT, United Kingdom

APPENDIX 3. — *Hongshanxi xiei* n. gen., n. sp., additional cranial features visible from CL scan images. Download this video file from:
http://sciencepress.mnhn.fr/sites/default/files/documents/fr/g2019v41a16-1-video.mp4

Downloaded From: https://bioone.org/journals/Geodiversitas on 18 Nov 2019
Terms of Use: https://bioone.org/terms-of-use Access provided by University College London